Brain/MINDS Beyond Human Brain MRI Project: A Protocol for Multi-Site Harmonization across Brain Disorders Throughout the Lifespan

Running Head: Brain/MINDS Beyond MRI study

Shinsuke Koike, M.D., Ph.D.[1,2,3,4]; Saori C Tanaka, Ph.D.[5]; Tomohisa Okada, M.D., Ph.D.[6]; Toshihiko Aso, M.D., Ph.D.[7]; Michiko Asano, Ph.D.[1]; Norihide Maikusa, Ph.D.[1,8]; Kentaro Morita, M.D., Ph.D.[9]; Naohiro Okada, M.D., Ph.D.[2,4,10]; Masaki Fukunaga, Ph.D.[11]; Akiko Uematsu, Ph.D.[1]; Hiroki Togo, MSc.[8]; Atsushi Miyazaki, Ph.D.[12]; Katsutoshi Murata, MSc.[13]; Yuta Urushibata, MSc.[13]; Joonas Autio, Ph.D.[7]; Takayuki Ose, MSc[7]; Junichiro Yoshimoto, Ph.D.[5]; Toshiyuki Araki, M.D., Ph.D.[14]; Matthew F Glasser, M.D., Ph.D.[15,16]; David C Van Essen, Ph.D.[15]; Megumi Maruyama, Ph.D.[17]; Norihiro Sadato, M.D., Ph.D.[11]; Mitsuo Kawato, Ph.D.[5,18]; Kiyoto Kasai, M.D., Ph.D.[2,3,4,10]; Yasumasa Okamoto, M.D., Ph.D.[19]; Takashi Hanakawa, M.D., Ph.D.[8,20]; Takuya Hayashi, M.D., Ph.D.[7]; Brain/MINDS Beyond Human Brain MRI Group

1) Center for Evolutionary Cognitive Sciences (ECS), Graduate School of Art and Sciences, The University of Tokyo, Meguro-ku, Tokyo 153-8902, Japan
2) University of Tokyo Institute for Diversity & Adaptation of Human Mind (UTIDAHM), Meguro-ku, Tokyo 153-8902, Japan
3) University of Tokyo Center for Integrative Science of Human Behavior (CiSHuB), 3-8-1 Komaba, Meguro-ku, Tokyo 153-8902, Japan
4) The International Research Center for Neurointelligence (WPI-IRCN), Institutes for Advanced Study (UTIAS), University of Tokyo, 7-3-1 Hongo, Bunkyo-ku, Tokyo 113-8654, Japan
5) Brain Information Communication Research Laboratory Group, Advanced Telecommunications Research Institutes International (ATR), Kyoto 619-0288, Japan
6) Human Brain Research Center, Kyoto University, Kyoto 606-8507, Japan
7) Laboratory for Brain Connectomics Imaging, RIKEN Center for Biosystems Dynamics Research, Hyogo 650-0047, Japan
8) Integrative Brain Imaging Center, National Center of Neurology and Psychiatry, Kodaira-shi, Tokyo 187-8551, Japan
9) Department of Rehabilitation, Graduate School of Medicine, The University of Tokyo, Bunkyo-ku, Tokyo 113-8655, Japan
10) Department of Neuropsychiatry, Graduate School of Medicine, The University of Tokyo, Bunkyo-ku, Tokyo 113-8655, Japan
11) Division of Cerebral Integration, Department of System Neuroscience, National Institute for Physiological Sciences, Okazaki 444-8585, Japan
12) Tamagawa University Brain Science Institute, 6-1-1 Tamagawagakuen, Machida, Tokyo 194-8610, Japan
13) Siemens Healthcare K.K. Shinagawa-ku, Tokyo 141-8644, Japan
14) Department of Peripheral Nervous System Research, National Institute of Neuroscience, National Center of Neurology and Psychiatry, Kodaira, Tokyo 187-8551, Japan
15) Department of Neuroscience, Washington University School of Medicine, St Louis, Missouri USA

16) Department of Radiology, Washington University School of Medicine, St Louis, Missouri, USA
17) Research Enhancement Strategy Office, National Institute for Physiological Sciences, Okazaki 444-8585, Japan
18) Center for Advanced Intelligence Project, RIKEN, Tokyo 103-0027, Japan
19) Department of Psychiatry and Neurosciences, Hiroshima University, Hiroshima 734-8551, Japan
20) Department of Integrated Neuroanatomy and Neuroimaging, Kyoto University Graduate School of Medicine, Kyoto 606-8303, Japan

Corresponding to:
Takuya Hayashi, M.D., Ph.D.
Laboratory for Brain Connectomics Imaging,
RIKEN Center for Biosystems Dynamics Research
6-7-3 Minatojima-minami-machi, Chuo-ku, Kobe, Hyogo 650-0047
E-mail: takuya.hayashi@riken.jp
Tel: +81-78-304-7140
Fax: +81-78-304-7141

Abstract

Psychiatric and neurological disorders are afflictions of the brain that can affect individuals throughout their lifespan. Many brain magnetic resonance imaging (MRI) studies have been conducted; however, imaging-based biomarkers are not yet well established for diagnostic and therapeutic use. This article describes an outline of the planned study, the Brain/MINDS Beyond human brain MRI project (FY2018 ~ FY2023), which aims to establish clinically-relevant imaging biomarkers with multi-site harmonization by collecting data from healthy traveling subjects (TS) at 13 research sites. Collection of data in psychiatric and neurological disorders across the lifespan is also scheduled at 13 sites, whereas designing measurement procedures, developing and analyzing neuroimaging protocols, and databasing are done at three research sites. The Harmonization protocol (HARP) was established for five high-quality 3T scanners to obtain multimodal brain images including T1 and T2-weighted, resting state and task functional and diffusion-weighted MRI. Data are preprocessed and analyzed using approaches developed by the Human Connectome Project. Preliminary results in 30 TS demonstrated cortical thickness, myelin, functional connectivity measures are comparable across 5 scanners, providing high reproducibility and sensitivity to subject-specific connectome. A total of 75 TS, as well as patients with various psychiatric and neurological disorders, are scheduled to participate in the project, allowing a mixed model statistical harmonization. The HARP protocols are publicly available online, and all the imaging, demographic and clinical information, harmonizing database will also be made available by 2024. To the best of our knowledge, this is the first project to implement a rigorous, prospective harmonization protocol with multi-site TS data. It explores intractable brain disorders across the lifespan and may help to identify the disease-specific pathophysiology and imaging biomarkers for clinical practice.

Keywords

Multi-site Study; HCP-style Brain Imaging; Psychiatric Disorders; Neurological Disorders; Harmonization Protocol; Traveling Subjects

Text

Abbreviations

DALYs, disability-adjusted life years
MRI, magnetic resonance imaging
HCP, Human Connectome Project
ABCD, Adolescent Brain Cognitive Development
BPD, bipolar disorder
MDD, major depressive disorder
DecNef, Decoded Neurofeedback
ASD, autism spectrum disorder
ADNI, Alzheimer's Disease Neuroimaging Initiative
AD, Alzheimer's disease
MCI, mild cognitive impairment
PPMI, Parkinson's Progression Markers Initiative
PD, Parkinson's disease
T1w, T1-weighted
T2w, T2-weighted
rsfMRI, resting state functional MRI
CRHD, Connectome Related to Human Disease
GLM, general linear model
TS, traveling subject
AMED, Japan Agency for Medical Research and Development
Brain/MINDS Beyond, Strategic International Brain Science Research Promotion Program
HARP, Harmonization protocol
DWI, diffusion-weighted imaging
QC, quality control
MNI, Montreal Neurological Institute
MSM, multi-modal surface matching
GLMM, general linear mixed model
CIFTI, Connectivity Informatics Technology Initiative
FEF, frontal eye field
PEF, premotor eye field
PSL, peri-sylvian language
STS, superior temporal sulcus
NODDI, nerite orientation and density imaging

126 **1. Introduction**

127 Psychiatric and neurological disorders are afflictions of the brain that can affect individuals
128 throughout their lifespans. Using the disability-adjusted life years (DALYs), which is a measure
129 of disease burden proposed by the World Health Organization Global Burden of Disease study,
130 in 2010 mental and behavioral disorders accounted for 7.4% of the total DALYs and
131 neurological disorders accounted for 3.0% (Murray et al., 2012), up from 5.4% and 1.9% in
132 1990, respectively. Since the 1990s, technical advances in magnetic resonance imaging (MRI)
133 have allowed detailed analysis of the organization of brain function and structure in humans.
134 Recent high-quality MRI studies with a large cohort are expected to provide neurobiological and
135 life-span information in healthy subjects (Glasser et al., 2016b; Harms et al., 2018; Miller et al.,
136 2016), which will hopefully provide diagnostic utility for patients with psychiatric and
137 neurological disorders (Drysdale et al., 2017; Elliott et al., 2018b; Koutsouleris et al., 2015;
138 Nunes et al., 2018). However, the diagnostic value of brain MRI in psychiatric disorders has not
139 yet been established, presumably because effect sizes tend to be small and overlap with
140 variability in healthy individuals (Yamashita et al., 2019). Protocols of scanning and analysis
141 have rarely been standardized across projects, though that has begun to change - especially for
142 large projects such as the Human Connectome Project (HCP; (Van Essen et al., 2012)), UK
143 Biobank (Miller et al., 2016), and the Adolescent Brain Cognitive Development (ABCD) project
144 (Casey et al., 2018).

145

146 *1.1. Previous multi-site neuroimaging studies for neuropsychiatric disorders*

147 Several brain imaging projects have attempted to identify suitable biomarkers in
148 neuropsychiatric diseases. Recent multi-site neuroimaging mega studies have revealed well-

149 replicated and clinically applicable findings from structural images; the Enhancing
150 NeuroImaging Genetics through Meta-Analysis Consortium in the U.S. (n = 4,568) and the
151 Cognitive Genetics Collaborative Research Organization in Japan (n = 2,564) replicated findings
152 that patients with schizophrenia have volumetric alterations of subcortical structures when
153 compared to healthy controls (Okada et al., 2016; van Erp et al., 2016). The findings were partly
154 evident in other psychiatric disorders, such as bipolar disorder (BPD) and major depressive
155 disorder (MDD) (Hibar et al., 2018; Schmaal et al., 2017; Schmaal et al., 2016; van Erp et al.,
156 2016). Using resting-state functional MRI (rsfMRI), a multi-site study successfully developed
157 generalized classifiers for psychiatric disorders. The Decoded Neurofeedback (DecNef) Project
158 (https://bicr.atr.jp/decnefpro/), a multi-site neuroimaging study in Japan (12 sites, n = 2,409),
159 developed a generalized classifier for autism spectrum disorder (ASD) with a high accuracy—
160 not only for the data in three Japanese sites (85%) but also for the Autism Brain Imaging Data
161 Exchange dataset (75%) (Yahata et al., 2016). The project also quantified the spectrum of
162 psychiatric disorders by applying the ASD classifier to other multi-disorder datasets
163 (schizophrenia, MDD, and attention-deficit/hyperactivity disorder). Therefore, the focus of
164 mega-analyses is shifting from features found in case-control studies to cross-disease
165 comparisons that can identify common and disease-specific features.
166 In the field of neurodegenerative disease, the Alzheimer's Disease Neuroimaging
167 Initiative (ADNI) is one of many major multi-site neuroimaging and biomarker studies of
168 Alzheimer's disease (AD) and mild cognitive impairment (MCI) that was started in 2005 in
169 North America (Mueller et al., 2005; Weiner et al., 2015). It contributed to the development of
170 blood and imaging biomarkers, the understanding of the biology and pathology of aging, and to
171 date has resulted in over 1,800 publications. ADNI also impacted worldwide ADNI-like

172 programs in many countries including Japan, Australia, Argentina, Taiwan, China, Korea,
173 Europe, and Italy. The Japanese ADNI (J-ADNI) conducted a multi-site neuroimaging study on
174 cognitively normal elderly patients, MCI, and mild AD (n = 537), which emphasized the
175 harmonization of the protocol and procedures with the ADNI (Iwatsubo et al., 2018). J-ADNI
176 also developed machine learning techniques using feature-ranking, a genetic algorithm, and a
177 structural MRI-based atrophy measure to predict the conversion from MCI to AD (Beheshti et
178 al., 2017). Inspired by the Parkinson's Progression Markers Initiative (PPMI; (Parkinson
179 Progression Marker Initiative, 2011), the Japanese (J-) PPMI team has also started a cohort in
180 patients with rapid eye movement sleep behavioral disorder, which is regarded to be prodromal
181 to Parkinson's disease (PD) (Mukai and Murata, 2017).
182 These previous mega-studies have contributed to the discovery of potential mechanisms
183 and biomarkers of multiple brain disorders. However, most of these imaging biomarkers have a
184 relatively small effect sizes and the study results were drawn from multi-site data which are often
185 heterogenous and used now outdated traditional low-resolution data acquisition protocols. In
186 addition, there have been no human brain MRI studies that explore multiple psychiatric and
187 neurological disorders that occur through the lifespan within the same cohort of subjects.
188
189 *1.2. High-quality multi-modal MRI protocols and preprocessing pipelines*
190 The HCP developed a broad approach to improving brain imaging data acquisition,
191 preprocessing, analysis, and sharing (Glasser et al., 2016b). It includes: 1) high-quality multi-
192 modal data acquisition; 2) in a large number of subjects; and 3) high-quality data preprocessing
193 and has proven usefulness of MRI techniques for understanding the detailed organization of a
194 healthy human brain (Elliott et al., 2018a; Glasser et al., 2016a; Smith et al., 2015). The HCP

195 aimed to delineate the brain areas and characterize neural pathways that underlie brain function
196 and behavior in 1,200 healthy young adults (Van Essen et al., 2012). HCP scans were performed
197 by a single MR scanner (a customized 3T Skyra, Siemens Healthcare GmbH, Erlangen,
198 Germany) in a total of 4-hour scan time for high-resolution multi-modal data, which included
199 T1-weighted (T1w) images, T2-weighted (T2w) images, diffusion-weighted images (DWI),
200 rsfMRI, and task fMRI (Glasser et al., 2016b; Glasser et al., 2013). The HCP also developed a
201 set of preprocessing pipelines with improved cross-subject alignment that dramatically improves
202 the spatial localization of brain imaging findings and also increasing statistical sensitivity
203 (Coalson et al., 2018; Glasser et al., 2013; Robinson et al., 2018). For the Lifespan Developing
204 and Aging HCP Projects (HCP-D and HCP-A) the original HCP protocol for healthy young
205 adults was shortened, for children and the elderly (60 to 90 min scan time; (Bookheimer et al.,
206 2019; Harms et al., 2018; Somerville et al., 2018), and for psychiatric and neurological disorders
207 (the Connectomes Related to Human Disease [CRHD];
208 https://www.humanconnectome.org/disease-studies), and adolescent development (the ABCD
209 project; (Casey et al., 2018). The UK Biobank used an even more abbreviated scanning approach
210 to collect a much larger number of cohort (n = 100,000) to predict health conditions (Miller et
211 al., 2016).
212 Many of these high-quality multimodal projects have been based on a single or small
213 number of the same model scanners at different sites and thus did not fully address
214 standardization of the data acquisition across different scanner models or vendors. We aim to
215 accelerate harmonization technologies to be used in at least five scanner platforms by combining
216 approaches to high-quality imaging acquisition, preprocessing, study design, and statistical bias
217 correction to potentially improve the sensitivity and validity of imaging biomarkers.

1.3. Traveling subjects

A harmonization approach is required for individual-based statistics using a multi-site dataset, even when the brain images are obtained using the same machine and protocol, because the data from each site has the bias from hardware and scanning protocol (measurement bias) and sampling variability (i.e. age, sex, handedness, and socioeconomic status). If measurement biases were correlated or anti-correlated with a specific disease state this would result in a positive or negative bias in a given measure, whereas uncorrelated biases would merely reduce sensitivity (i.e. SNR) of the measure. Sampling biases due to biological differences in the sampled populations should also be considered for both case and control groups. Data harmonization has been proposed to control for these biases, including a general linear model (GLM) with the site as the covariate, a Bayesian approach (Fortin et al., 2018; Fortin et al., 2017), and a meta-analytic approach (Okada et al., 2016; van Erp et al., 2016), but the methods used for controlling both biases are unable to distinguish between them (Yamashita et al., 2019). Inter-site cross-validation by machine learning and deep learning techniques is a method that aims to remove bias without any specific preparation if large-sample datasets are available (Nunes et al., 2018). However, this method extracts stable characteristics across the images and is limited to using only a part of the information for further analysis. In addition, it is unclear whether the classifiers obtained by such methods can be applied to an independent new site of the initial multi-site project.

The traveling subject (TS) approach is a powerful research design to control for site differences (Figure 1). This approach requires the images from the same participants at all the participating sites, but also requires significant effort from the sites and the participants when

241 compared to other harmonization methods listed above, and the TS scans must be completed
242 before the analysis starts. However, the TS approach can differentiate most of the sample
243 variability from measurement bias in functional MRI (Yamashita et al., 2019), structure and
244 diffusion MRI (Tong et al., 2020). The DecNef Project explored rsfMRI functional connectivity
245 for multiple psychiatric diseases and scanned nine TS participants who received repeated MRI
246 measurements at all sites. Measurement and sampling biases for each group (schizophrenia,
247 MDD, ASD, and healthy controls) were segregated from individual and disease-specific factors
248 as the rest of sampling variability. The results showed that the effects of both bias types on
249 functional connectivity were greater than or equal to those of disease-specific factors. With
250 regard to measurement bias, differences in phase encoding direction had the biggest effect size
251 when compared to those of vendor, coil, and scanner within the same vendor. The harmonization
252 method was estimated to reduce measurement bias by 29% and improve the signal-to-noise ratio
253 by 40% (Yamashita et al., 2019). Further investigations are needed to determine the best
254 approach for reducing sampling bias arising from biological differences in the sampled
255 population.
256

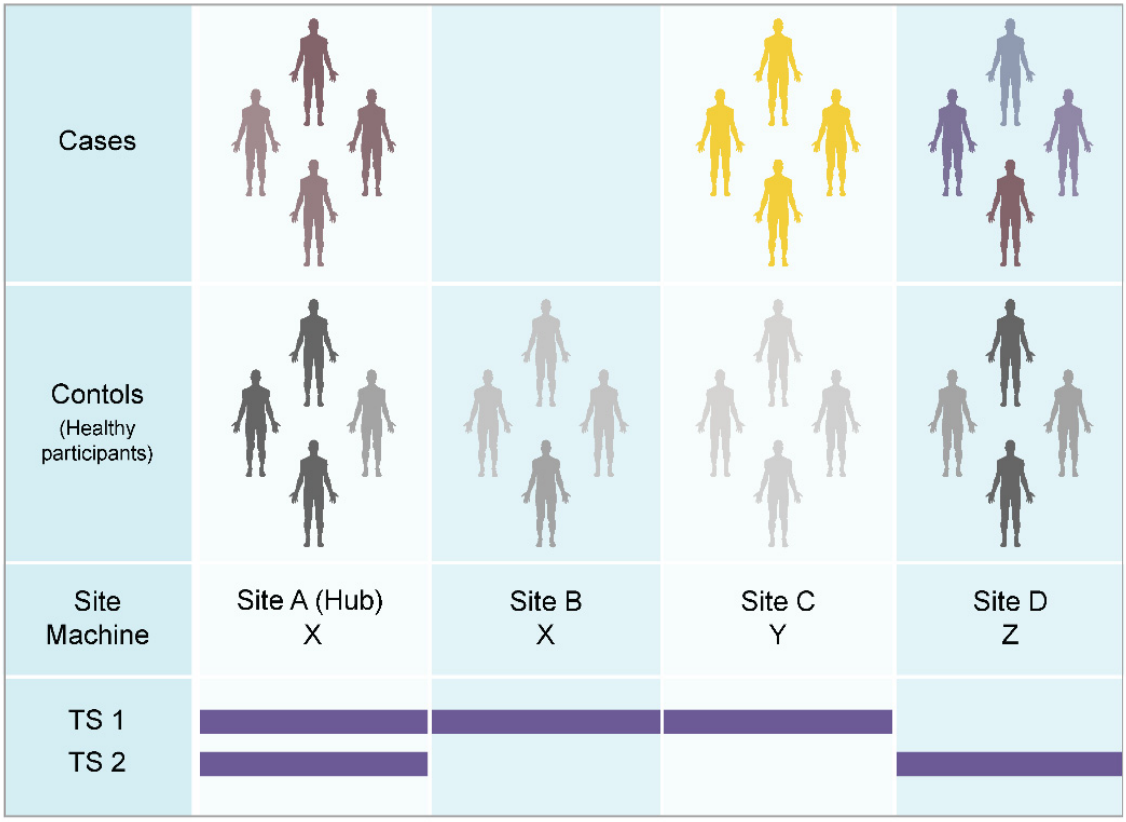

Figure 1. Case-control studies and traveling subject approach.
(Top) When we analyze multi-site data from a set of case-control MRI studies, we must consider machine and protocol-derived bias (measurement bias) as well as sampling bias (from biological differences in the sampled populations). Even if the machine and protocol are the same between sites (e.g. Sites A and B), measurement bias may still occur because of slight differences in the magnetic or radiofrequency fields, etc. Sampling bias should be considered for patient groups as well as control groups, given that the control participants were recruited according to the demographics in the patient group. (Bottom) The traveling subject (TS) harmonization approach enables us to combine with case-control datasets by differentiating between measurement and sampling biases (Yamashita et al., 2019). Based on the general linear model (GLM), TS participants need to receive measurements from all participating sites (e.g. only TS 1 dataset). To reduce the effort of TS participants and participating sites, this project applies a general linear mixed model (GLMM) approach and hub-and-spoke model to the TS project. With this approach, all participants receive scans at one or more hub sites (site A), and measurement bias is calculated using multiple TS datasets by means of a GLMM (TS 1 and 2).

1.4. Brain/MINDS Beyond project

The Strategic International Brain Science Research Promotion Program (Brain/MINDS Beyond; FY2018–FY2023; https://brainminds-beyond.jp/) was funded by the Japan Agency for Medical Research and Development (AMED) to support global brain research by enhancing collaboration with the domestic projects of other countries. Brain/MINDS Beyond consists of four research groups: G1-1, Identification of the pathogenic mechanism of psychiatric and neurological disorders through the acquisition and analysis of brain MRI-scan images and clinical data (Developmental [G1-1D], adult [G1-1A], and senescent [G1-1S] stages); G1-2, Brain MRI data acquisition, analysis, and informatics; G2, Research involving an inter-species comparison of human and nonhuman primate brains by structural and functional parcellation and homology analyses; and G3, Development and application of technologies, such as neuro-feedback through collaboration with artificial intelligence research projects as well as the Innovative Research Group. In human brain imaging, G1-1 intends to measure human participants, including patients with neuropsychiatric disorders, across the lifespan, and G1-2 intends to coordinate and support data acquisition, storage, preprocessing, analysis, and distribution (Figure 2 and Table 1). The Brain/MINDS Beyond MRI working group also set up a standardized procedure for MRI data acquisition (Harmonization protocol [HARP]) and clinical and neurocognitive data assessment (Tables 2 and 3). Following previous multi-site studies in Japan (Iwatsubo et al., 2018; Okada et al., 2016; Yahata et al., 2016; Yamashita et al., 2019), the overall goal of this project is expected to find altered brain imaging characteristics in psychiatric and neurological disorders that can be applied to future therapeutic investigations and clinical devices. To address limitations of previous findings in multi-site studies, we are using high performance research-based MRI scanners and we modeled our multi-modal protocol (T1w images, T2w images, diffusion-weighted imaging [DWI], rsfMRI, task fMRI, quantitative susceptibility mapping, and arterial

spin labeling) on that used by the HCP and ABCD study projects. We are also obtaining a TS dataset for the harmonization of the clinical MRI datasets and the development of technical tools to harmonize the multi-site data. Once the project period ends, the data will be openly distributed to researchers via a public database.

Here, we introduce the Brain/MINDS Beyond human brain MRI project and show preliminary results in high-quality neuroimaging using the TS data that is amenable to harmonization. We then discuss our plans for investigating the neural basis of psychiatric and neurological disorders in the hope of developing therapeutic targets and devices that are applicable to clinical settings.

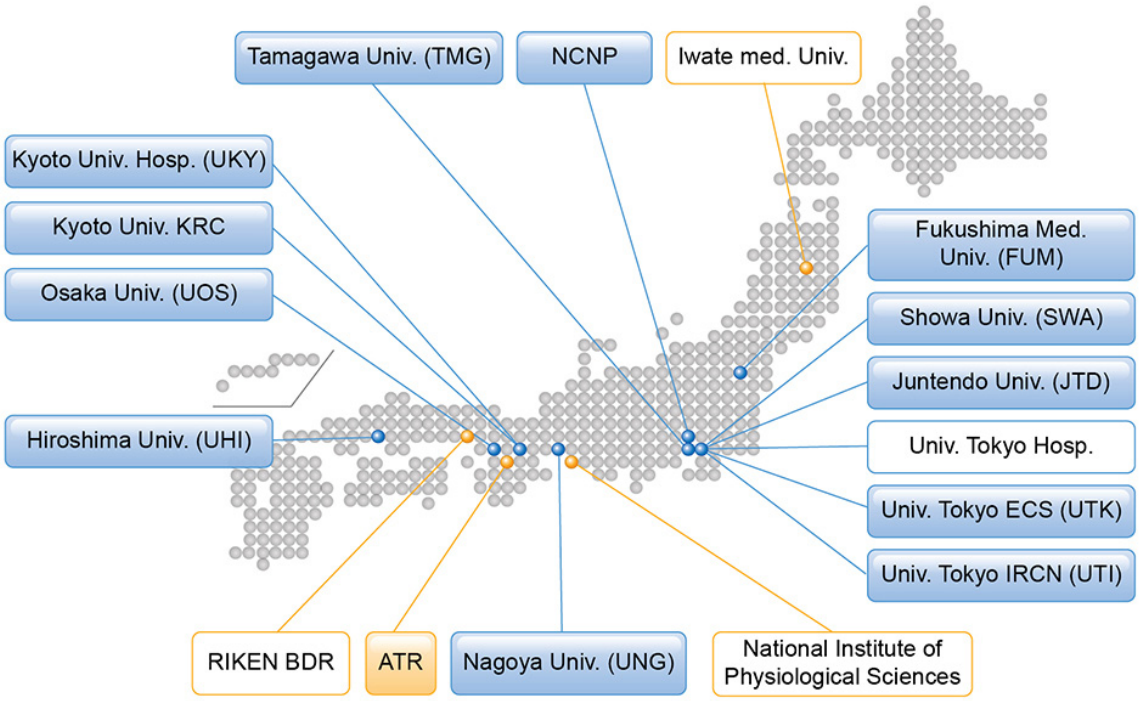

Figure 2. Brain/MINDS Beyond human brain MRI project.
Institutes in the blue boxes show measurement and analysis sites for neuropsychiatric disorders, and those in the orange boxes show analysis support sites. Institutes listed in boxes with a colored background represent participation in the traveling subject project.

2. Brain/MINDS Beyond human brain MRI study

2.1. Participating sites and target population

As of March 2020, 13 sites have approved this study project, received approval from their respective ethical review board(s), and obtained clinical and TS measurements using the appropriate MRI scanners (Table 1). Of these, 5 sites mainly explore psychiatric disorders (schizophrenia, ASD, MDD, and BPD), 4 sites neurological disorders (AD, PD, multiple system atrophy, progressive supranuclear palsy, chronic pain disorder, and epilepsy), and 2 sites both categories. Two sites measure the general adolescent population to investigate brain development and recruit through advertisement and cohort studies (Ando et al., 2019; Okada et al., 2019). Each site intends to obtain brain images and demographic (and clinical) characteristics for clinical cases and match controls for age, sex, premorbid IQ or educational attainment, socio-economic status, and handedness (See Cognitive and behavioral assessment section). The exclusion criteria were set by each study purpose (i.e. low premorbid IQ, history of loss of consciousness for more than 5 min, illegal drug use, and alcohol dependency). Illegal drug use can be a major concern for disease onset and poor prognosis, especially for psychiatric disorders. However, there is far less illegal drug use in Japan compared to Western European countries (Degenhardt et al., 2008; Lee and Kwon, 2016), and most of the participating sites excluded those with a current illegal drug use or previous history of regular use (Koike et al., 2013).

For the TS project, 75 healthy adults planned to undergo 6 to 8 scans at three or more sites within 6 months (See Traveling Subject Project section). Five or more participants per site were recruited. Each participant received test-retest scans at the recruitment site and underwent scans at different sites including a hub site. We set up three hub sites, according to a hub-and-

spoke model, in which all participants received scans using a MAGNETOM Prisma scanner (Siemens Healthcare GmbH, Erlangen, Germany) and the CRHD and HARP protocols.

Table 1. Participating sites of the Brain/MINDS Beyond MRI project.

Site	Research group	Role for the project	Role for TS	MRI scanner (System version)	Protocol	Main target population
UTK	G1-1D, G1-2	Data acquisition/Analysis	Hub	Prisma (VE11C)	CRHD	Adolescent cohort, HP, ASD, Sch, MDD, Epilepsy
UTI	G1-1D, G1-2	Data acquisition/Sharing	Hub	Prisma (VE11C)	CRHD	HP, ASD, Sch, MDD, BPD
ATR	G1-2, G3	Data acquisition/Sharing/ Analysis	Hub	Prisma (VE11C)	CRHD	HP
FUM	G1-1S	Data acquisition	Spoke	Skyra (VE11C)	HARP	HP, AD, PD
TMG	G1-1D	HARP setup/Data acquisition	Spoke	Trio (VB19A)	HARP	Adolescent cohort
SWA	G1-1D, G3, IR	HARP setup/Data acquisition	Spoke	Skyra (VE11E)	HARP	HP, ASD
NCNP	G1-1S	HARP setup/Data acquisition/Sharing/ Analysis	Spoke	Verio Tim+Dot (VD13A)	HARP	HP, Sch, MDD, AD, PD
JTD	IR	Data acquisition	Spoke	Prisma (VE11C)	HARP	HP, PD, MSA, PSP
UOS	G2	Data acquisition	Spoke	Prisma (VE11C)	HARP	HP, Chronic pain
UHI	G1-1A, G3	HARP setup/Data acquisition	Spoke	Skyra (VE11C)	HARP	HP, MDD, BPD
UNG	BM	Data acquisition	Spoke	Verio (VB17A)	HARP	HP, Sch
UKY	G1-1S	HARP setup/Data acquisition	Spoke	Skyra (VE11C)	HARP	HP, AD, PD
KRC	G1-1A	Data acquisition	Spoke	Verio (VB17A)	HARP	HP, Sch, MDD, BPD
BDR	G1-2	HARP setup/Data Analysis	Spoke	Prisma (VE11C)	HARP	NA

Abbreviations: UTK, The University of Tokyo ECS (Komaba Campus); UTI, The University of Tokyo IRCN; FUM, Fukushima Medical University; TMG, Tamagawa Academy & University; SWA, Showa University; NCNP, National Center of Neurology and Psychiatry; JTD, Juntendo Hospital; ATR, Advanced Telecommunications Research Institute International; UOS, Osaka University; UHI, Hiroshima University; UNG, Nagoya University; UKY, Kyoto University; KRC, Kyoto University Kokoro Research Center; BDR, RIKEN Center for Biosystems Dynamics Research; IR, Innovative Research Group in Brain/MINDS Beyond; BM, Brain/MINDS project; CRHD, Human Connectome Studies Related To Human Disease protocol; HARP, harmonization protocol; HP, healthy participants; ASD, autism spectrum disorders; Sch, schizophrenia; MDD, major depressive disorder; BPD, bipolar disorder; AD, Alzheimer's disease; PD, Parkinson disease; MSA, multiple system atrophy; PSP, progressive supranuclear palsy.

330 *2.2. Harmonized brain MRI protocols*

331 We developed protocols that minimize potential differences related to measurement and increase
332 the MR image sensitivity to brain organization in psychiatric and neurological disorders. From a
333 neurobiological perspective, the cerebral cortex is organized by a 2D sheet-like structure with an
334 average thickness of 2.6 mm embedded and folded in the ~1300 mL of brain volume (Glasser et
335 al., 2016b). From a neuroimaging perspective, the spatial resolution and homogeneity of the
336 images are important factors that may induce bias and error during the image analysis; these
337 include partial voluming, image distortion, errors in brain segmentation, and registration. Of
338 these, respecting spatial fidelity of neuroanatomical structures is the most important approach for
339 achieving unbiased imaging (Glasser et al., 2016b). Therefore, the spatial resolution of the
340 imaging was determined based on cortical thickness and was matched across all scanners. The
341 phase encoding direction of EPI-based functional and diffusion MRI is an important factor that
342 relates to spatial distortion (and signal loss in fMRI) in association with the polarity of the
343 direction, echo spacing, and B0 magnetic field homogeneity; therefore, we acquire a spin-echo
344 filed map with opposite phase encoding directions to enable distortion correction (Andersson et
345 al., 2003). Based on these strategies, two MRI protocols were planned for use in the project: 1) a
346 harmonized MRI protocol (HARP), which can be run on the multiple MRI scanners/sites within
347 a period of 22 to 65 min; and 2) an 'HCP style' MRI protocol used by HCP CRHD for the high-
348 performance 3T MRI scanner (e.g. MAGNETOM Prisma).

349 The HARP was created to be used at multiple MRI scanners/sites, and it was designed to
350 obtain high-quality and standardized brain MRI data in a 'clinically' practical window of time
351 (Table 2 and Supplementary Table S1). The parameters of the MRI scanners were as follows: 1)
352 static magnetic field strength of 3T; 2) multi-array head coil with 32 or more channels; and 3)

353 ability to perform a multi-band EPI sequence provided from Center for Magnetic Resonance
354 Research, University of Minnesota with an acceleration factor of 6 (Moeller et al., 2010;
355 Setsompop et al., 2012; Xu et al., 2013). In 2019, the protocol was adapted for use with five MRI
356 scanners/systems (MAGNETOM Prisma, Skyra, Trio A Tim, Verio, and Verio Dot; Siemens
357 Healthcare GmbH, Erlangen, Germany), and we plan to expand it to different MRI
358 scanners/vendors during the project period and in fact we are working on creating HARP
359 protocol for GE scanners. The HARP was intended to perform the brain scan within a period of ~
360 30 min using a high-resolution structural MRI scan (T1w and T2w, spatial resolution of 0.8 mm)
361 and two high-sensitive rsfMRI scans with opposing phase directions, a spatial resolution of 2.4
362 mm, and a temporal resolution of 0.8 s for a total of 10 minutes. The protocols also include
363 optional sequences for four additional rsfMRI scans, task fMRI (Emotion and CARIT) (Winter
364 and Sheridan, 2014), two DWI scans with opposing phase encoding directions, quantitative
365 susceptibility mapping, and arterial spin labeling. The minimum and maximum scanning time of
366 the HARP is 22 and 65 min, respectively (Table 2). The preliminary results across scanners and
367 multi-array coils in the same subject (ID = 9503) revealed that the temporal signal-to-noise ratio
368 (tSNR) was very high in all the scanners. The mean ± standard deviation across 32k
369 greyordinates was 161 ± 80 in the Prisma at UTK, 155 ± 81 in the Verio Dot at SWA, 151 ± 72
370 in the Skyra fit at SWA, 151 ± 80 in the Verio at ATR, and 150 ± 74 in the Prisma fit at ATR;
371 the values and their distributions were similar across scanners/sites (Figure 3A).
372 The CRHD protocol was planned for collaboration with the HCP CRHD for the Early
373 Psychosis Project. The HCP CRHD protocol also included high-resolution structural MRI
374 (spatial resolution of 0.8 mm), high-resolution resting-state fMRI (spatial resolution of 2 mm)

375 with an opposing phase encoding direction and longer scan time, and high-resolution and high
376 angular diffusion MRI.

377 The installation of the protocols in the MRI scanners was ensured by conducting
378 hierarchical parameter checks and site visits at the beginning of the measurement period. After
379 the protocol installation, each site sent XML files of the installed protocol from the MRI scanner
380 to the protocol management site (UTK), and all the parameters were confirmed with a checksum
381 algorithm using R (R Core Team, 2018). This process was useful for validating the protocols
382 across sites/scanners because some of the MRI scanners actually underwent inappropriate
383 installation and were set with different parameters. The results were then sent back to the
384 collaborators, who edited the parameters. We also checked the DICOM files that are deposited in
385 the ATR XNAT server. In this phase, we checked the parameters, slice numbers, and diffusion
386 gradient information (bvec and bval).

387 The manuals were shared and used at the sites for protocol installation, demographic and
388 clinical assessment before the scan (e.g. handedness), and the assessment of and instruction to
389 participants during the scan (e.g. general instruction during the scan, fixation to the cross during
390 rsfMRI scans, and the assessment of sleepiness during the rsfMRI).

391 **Table 2. CRHD and HARP protocols.**

Subset	Sequence	Duration			Participant instruction
		Prisma		Skyra, Trio, Verio Dot, Verio	
		CRHD	HARP	HARP	
rsfMRI 1	SEF AP	0:32	0:06		Fixation
	BOLD AP	5:46	5:08		Fixation
	SEF PA	0:32	0:06		Fixation
	BOLD PA	5:46	5:08		Fixation
Structure	T1 MPR	6:38	5:22		Rest
	T2 SPC	5:57	5:31	5:22-6:26	Rest
Subtotal		**25 min**	**22 min**	**22-23 min**	
ASL		NA	2:45[b]		Rest
QSM		NA	5:03[c]		Rest
DWI	AP	6:07	3:29	4:50	Rest
	PA	6:05	3:32	4:54	Rest
	AP	5:39	NA	NA	Rest
	PA	5:39	NA	NA	Rest
rsfMRI 2	See rsfMRI 1[a]	13 min	11 min		Fixation
rsfMRI 3	See rsfMRI 1[a]	NA	11 min		Fixation
Task fMRI EMOTION	SEF AP	NA	0.06		Task
	SEF PA	NA	0.06		Task
	BOLD PA	NA	4.08		Task
Task fMRI CARIT	SEF AP	NA	0.06		Task
	SEF PA	NA	0.06		Task
	BOLD PA	NA	4.08		Task
Total		**61 min**	**68 min**	**59-68 min**	

392 Abbreviations: rsfMRI, resting-state functional MRI; ASL, arterial spin labeling; QSM,
393 quantitative susceptibility mapping; DWI, diffusion weighted imaging; SEF, spin echo field
394 mapping; BOLD, blood oxygenation level dependent; T1 MPR, T1-weighted magnetization
395 prepared rapid acquisition with gradient echo; T2 SPC, T2-weighted sampling perfection with
396 application optimized contrasts using different flip angle evolutions.
397 a set of SEF AP, BOLD AP, SEF PA, and BOLD PA.
398 b Only for Prisma and Skyra.
399 c Only for Prisma, Skyra, and Verio Dot.

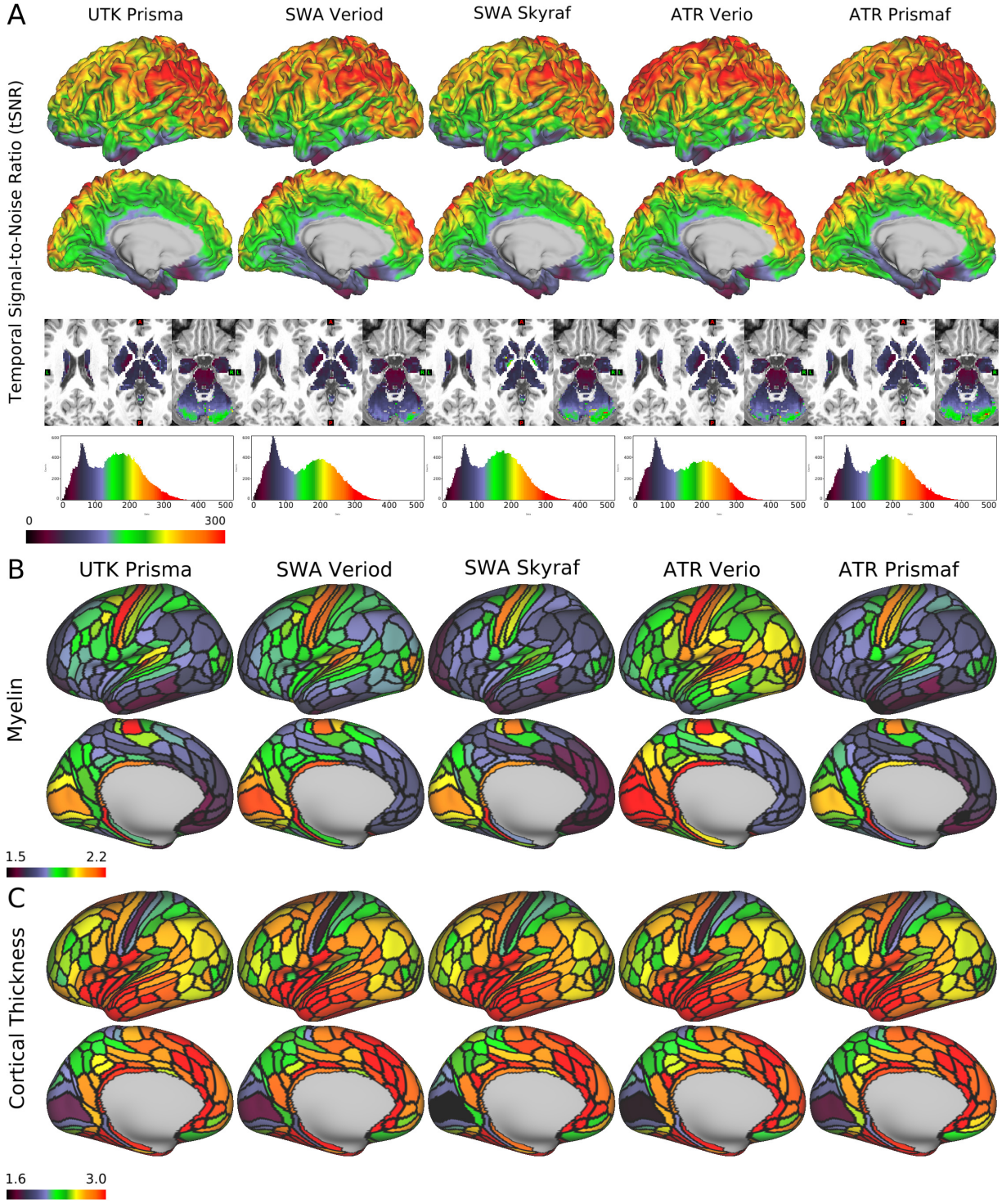

Figure 3. Quality of MRI and preliminary cortical structures obtained by HARP in a single traveling subject across scanners/sites.

A) Temporal signal-to-noise ratio (tSNR) obtained in a single subject (ID = 9503) across different scanners/sites by a harmonized MRI protocol (a sequence of functional MRI in HARP using a multi-band echo planar imaging with TR/TE = 800/34.4 ms; see Supplementary Table S1 for other details). The images from top to bottom show color-coded tSNR maps in 32k greyordinates (see main text) overlaid on the lateral and medial surface of the mid-thickness surface of the left hemisphere, the subcortical sections of the T1w image, and the histogram of the tSNR values. B) Cortical myelin contrast (T1w/T2w ratio) across different scanners. The myelin contrast is not corrected for the biasfield and parcellated by the HCP MMP v1.0 (Glasser et al., 2016a). C) The map shows cortical thickness across different scanners. Cortical thickness is corrected by curvature and parcellated by the HCP MMP v1.0. The tSNR, myelin map and cortical thickness are comparable across scanners. Data at https://balsa.wustl.edu/7q4P9 and https://balsa.wustl.edu/6Vvqv

2.3. Cognitive and behavioral assessment

Each participating site assesses demographic characteristics (i.e. age, sex, and socioeconomic status), clinical characteristics (i.e. diagnosis, symptom severity, cognitive function, and general functioning), and subjective social evaluations (i.e. quality of life and well-being) (Table 3). Each subgroup (G1-1D, G1-1A, G1-1S, and G1-2 TS) indicates standard scales, some of which are uniform across subgroups and easier to share and use when analyzing brain images.

407 **Table 3. Clinical and neuropsychological assessment.**

	G1-1D	G1-1A	G1-1S
Depression	K6 or BDI-II	BDI-II and PHQ-9	PHQ-9 and BDI-II/GDS-15
Anxiety	—	GAD-7	STAI
Autism	AQ-10, AQ-50 or SRS-2 (for developmental disorders)	AQ-10 or AQ-50	—
Psychosis	APSS	—	NPI-Q
Intellectual ability	JART-25 or WAIS-III (WISC at the age of 15 years or less) Information and Picture completion subtests	JART-25	JART-25
Cognitive function	CANTAB or BACS-J	CANTAB or BACS-J	ADAS-Cog11, CDT, CDR, FAB, HVLT-R, JLO, MMSE, MoCA-J, SDMT, TMT-A/B, WMS-R
General function and disability	GAF, mGAF or WHO-DAS 2.0	GAF, mGAF or WHO-DAS 2.0	Schwab & England ADL
Quality of life	EQ-5D	EQ-5D	PASE
Well-being	WHO-5	WHO-5	SHAPS
Handedness	EHRS or UTokyo	EHRS or UTokyo	UTokyo

408 Abbreviations: K6, 6-item Kessler Screening Scale for Psychological Distress; BDI-II, Beck
409 Depression Inventory－Second Edition; PHQ-9, Patient Health Questionnaire-9; GDS-15,
410 Geriatric Depression Scale 15; GAD-7, General Anxiety Disorder-7; STAI, State-Trait Anxiety
411 Inventory; AQ-10, 10-item short version of the Autism Spectrum Quotient; AQ-50, Autism
412 Spectrum Quotient (original version); APSS, Adolescent Psychotic-like Symptom Screener;
413 NPI-Q, Neuro Psychiatric Inventory-Brief Questionnaire Form; JART-25, 25-item short version
414 of the Japanese Adult Reading Test; WAIS-III, Wechsler Adult Intelligence Scale－Third
415 Edition; GAF, Global Assessment of Functioning; mGAF, modified GAF; WHO-DAS 2.0, the
416 World Health Organization Disability Assessment Schedule II; Schwab & England ADL,
417 Modified Schwab and England ADL (Activities of Daily Living) scale; CANTAB, Cambridge
418 Neuropsychological Test Automated Battery; BACS-J, the Brief Assessment of Cognition in
419 Schizophrenia Japanese version; ADAS-Cog, Alzheimer's Disease Assessment Scale-cognitive
420 component; CDT, Clock Drawing Test; CDR, Clinical Dementia Rating; FAB, Frontal
421 Assessment Battery; HVLT-R, Hopkins Verbal Learning Test-Revised; JLO, Judgment of Line
422 Orientation; MMSE, Mini-Mental State Examination; MoCA-J, Japanese version of Montreal
423 Cognitive Assessment; SDMT, Symbol Digit Modality Test; TMT-A/B, Trail Making Test Parts
424 A and B; WMS-R, Wechsler Memory Scale-Revised; EQ-5D, EuroQol 5 Dimension
425 questionnaire; WHO-5, World Health Organization-Five Well-Being Index; PACE, Physical
426 Activity Scale for Elderly; SHAPS, Snaith-Hamilton Pleasure Scale; EHI, Edinburgh
427 Handedness Inventory; UTokyo, 14-item Rating Scale of Handedness for Biological Psychiatry
428 Research among Japanese People.

429 *2.4. Travelling subject project*

430 Based on the previous study (Yamashita et al., 2019), we conduct a TS project for the CRHD and
431 HARP protocols. At some sites, we also scan TS with the previous protocol (named as SRPB
432 [Strategic Research Program for Brain science]), which was used in the multi-site studies to
433 achieve retrospective harmonization (Iwatsubo et al., 2018; Okada et al., 2016; Yahata et al.,
434 2016; Yamashita et al., 2019). Because we limit the scanners, head coils, and protocols in this
435 project, we expect to see reduced measurement biases, which may enhance the disease-related
436 effect size in clinical studies and provide better ways to diminish bias in future studies.

437 The previous data harmonization using the TS dataset was based on a GLM (Yamashita
438 et al., 2019), in which participants needed to travel to all the sites/scanners. In contrast, the
439 present TS project was designed so that the participants travel only some of the test
440 sites/scanners, and statistical harmonization flexibly adapt the incompleteness by using a general
441 linear mixed model (GLMM; Figure 1). This design may also adapt the incompleteness of the
442 scanning for each participant, since the current protocols require a longer scan time compared to
443 previous ones, and thus result in potential cancellation or data completeness. To ensure
444 harmonization across all the sites/scanners, we applied a hub-and-spoke model to arrange
445 traveling scans at each recruitment site (Supplementary Table S2). Each participant undergoes
446 CRHD and HARP scans using the Prisma (~2 hours) at one or more hub sites (UTK, UTI, and
447 ATR) to harmonize the data within the Brain/MINDS Beyond project and other projects (e.g.
448 Brain/MINDS, HCP, and ABCD) and test the difference in quality between the protocols. The
449 other visiting sites were determined in consideration of the site locations, machine differences,
450 and project similarities between the sites. Each participant receives multiple scans at the
451 recruitment site to assess the test-retest reliability (1-hour x 2 sessions).

For the TS project, 75 healthy adults—five or more participants per site—are scheduled to undergo 6 to 8 scans at three or more sites within 6 months (Supplementary Table S2). The total number of scans and spokes between the sites are expected to be 455 and 465, respectively (Figure 4A). As of March 2020, 74 participants were registered and 405 scans (89.0 %) were completed and uploaded to the ATR XNAT server. The data provided 368 spokes (76.1 %, Figure 4B). The TS project will end in August 2020.

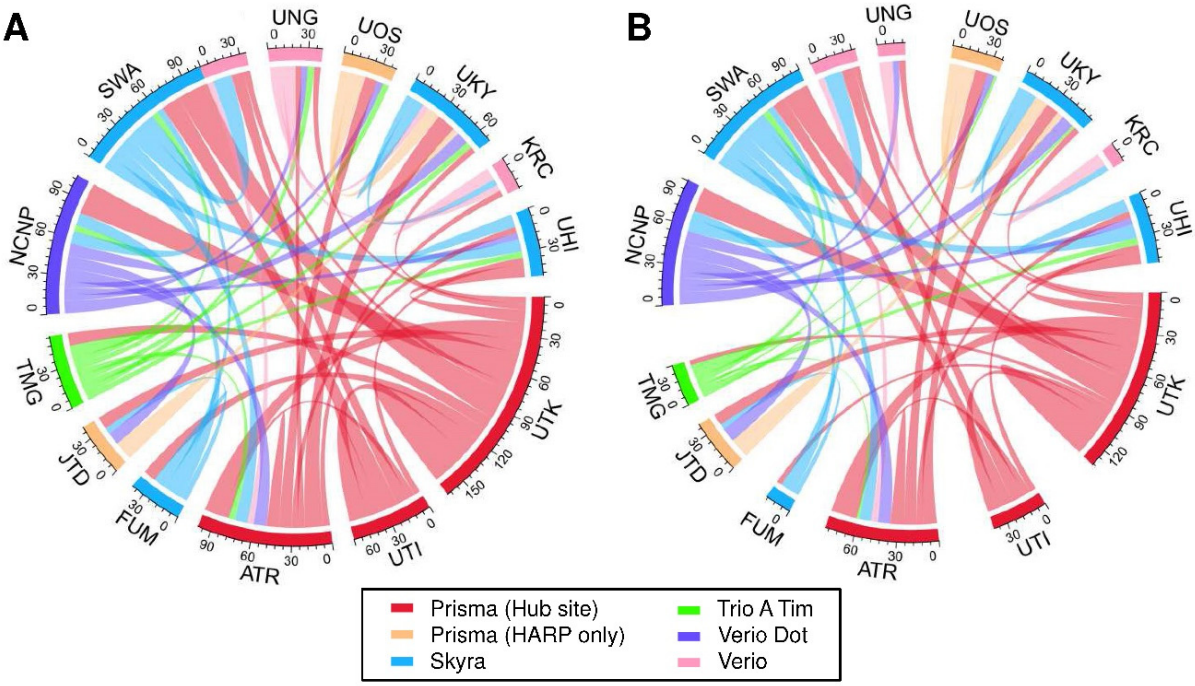

Figure 4. Expected and current data connection of the traveling subjects.
Data connections in the traveling subject project that were (A) initially planned and (B) the actual connections as of March 2020. Hub sites using Prisma and other sites using Prisma, Skyra, Trio A Tim, Verio Dot, and Verio are illustrated in red, orange, blue, green, purple, and pink, respectively.

2.5. Data storage, preprocessing, and quality control

2.5.1. Data logistics

462 Brain MR images obtained using the CRHD and HARP protocols in this study project and
463 related studies are stored, preprocessed, and distributed using the XNAT server system
464 (https://www.xnat.org/) (Figure 5). Due to the legacy of previous multi-site studies (Iwatsubo et
465 al., 2018; Yahata et al., 2016; Yamashita et al., 2019), several data centers were already available
466 for this project. The images obtained from the development and adult projects (G1-1D and G1-
467 1A) will be sent to an XNAT server at ATR and the clinical data will be sent to UTI. For the
468 senescent project (G1-1S), all the data will be sent to the NCNP (Iwatsubo et al., 2018). The TS
469 data will also be sent to the ATR server shown in dashed lines. When uploading to the XNAT
470 server, personal information (i.e. name and date of birth) contained in DICOM is automatically
471 removed using an anonymization script of XNAT. A defacing procedure is performed for T1w
472 and T2w images. These processes de-identify the MRI data. After manually checking whether
473 the face images are completely obscured, all the anonymized MRI data are shared using Amazon
474 AWS with RIKEN BDR, in which all image preprocessing is performed (See Preprocessing
475 pipelines section). Preprocessed data are sent back to the servers and can be seen with limited
476 access (i.e. participating sites). After a quality control (QC), cleaned imaging data with a
477 demographic and clinical datasheet will be stored in the distribution server(s). All data will be
478 also sent to backup server(s).

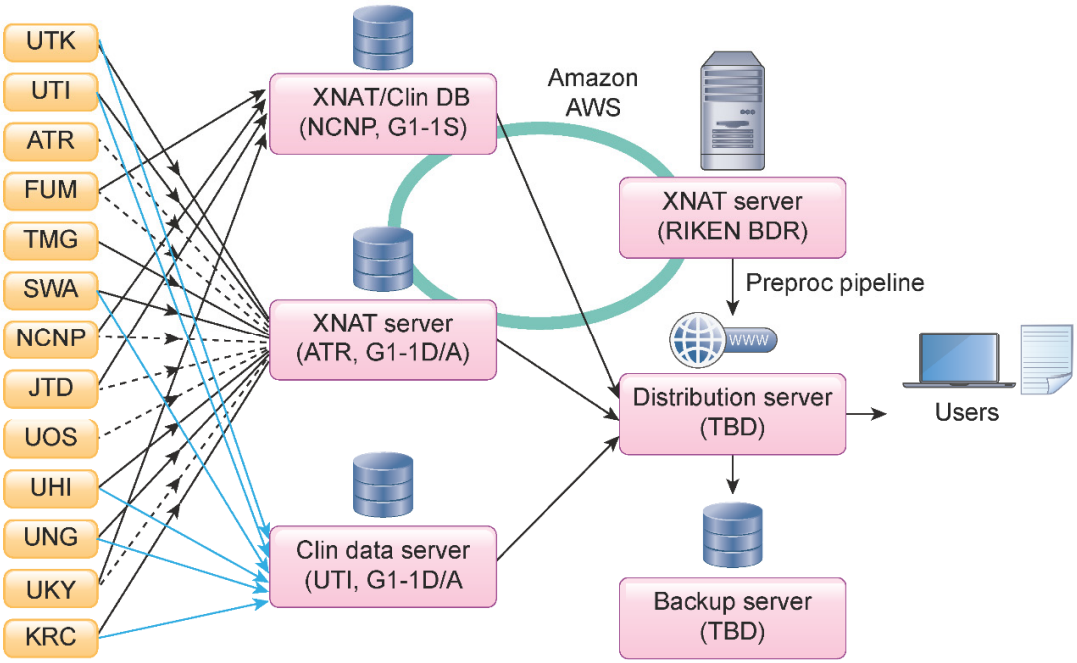

Figure 5. Data storage, preprocessing, quality check, and data sharing.
MRI (black line) and clinical (blue line) data from G1-1D and G1-1A sites are sent to the XNAT server and a data server at ATR and UTI, respectively. All data from G1-1S sites are sent to an XNAT server and a data server managed by NCNP, as this group applied a standard clinical assessment protocol to the project following a previous multi-site study. Traveling subject data from G1-1S sites are also sent to the XNAT server in ATR (dot line). XNAT servers at NCNP, ATR, and RIKEN BDR are linked by Amazon AWS to share the imaging data. NCNP manages a separate server for storing clinical data (Clin DB) being collected from the participants in this project. All MR images are preprocessed at RIKEN BDR. All MR images are preprocessed at RIKEN BDR. All the raw and preprocessed data will be stored and provided to the users in a distribution server. A backup server will be placed at a different site.

2.5.2. Preprocessing pipelines

All neuroimaging data are preprocessed at RIKEN BDR for this project. The MR images are sent via Amazon S3 to a high-throughput parallel computing system at RIKEN BDR for preprocessing. The raw MRI data in DICOM format are converted to those in NIFTI using a conversion program, BCILDCMCONVERT (https://github.com/RIKEN-BCIL/BCILDCMCONVERT), by which folder structures are created and all the imaging parameters are read and stored including the type of gradient, k-space read out time in phase and

487 read directions, phase encoding directions, to be used for preprocessing. The preprocessing is
488 performed using the HCP pipeline 4.2.0 (Glasser et al., 2013) with modifications for adapting
489 and harmonizing multiple scanners. In brief, the structural MRI (T1w and T2w) is first corrected
490 for image distortions related to the gradient nonlinearity in each scanner type and the
491 inhomogeneity of the B0 static magnetic field in each scan. The signal homogeneity is dealt with
492 by prescan normalization and is also improved by a biasfield correction using T1w and T2w
493 images (Glasser and Van Essen, 2011). The T1w and T2w images are fed into non-linear
494 registration to the Montreal Neurological Institute (MNI) space and used for cortical surface
495 reconstruction using FreeSurfer (Fischl, 2012), surface registration using multi-modal surface
496 matching (MSM) (Robinson et al., 2018) and folding pattern (MSMsulc); this is followed by the
497 creation of a myelin map using T1w divided by T2w and surface mapping (Glasser and Van
498 Essen, 2011). An example of a cortical myelin map (not biasfiled corrected [non BC]) in a single
499 subject (ID = 9503) across scanners/sites is parcellated by HCP MMP v1.0 (Glasser et al., 2016a)
500 and presented in Figure 3B, revealing the typical cortical distribution of the high myelin contrast
501 in the primary sensorimotor (aeras 1, 3a, 3b, 4), auditory (A1), visual (V1), middle temporal, and
502 ventral prefrontal (47m) areas—as demonstrated previously (Glasser and Van Essen, 2011). The
503 distributions over the cortex were comparable between scanners, although absolute values were
504 slightly different suggesting the residual bias from transmit field across scans/scanners (see also
505 2.5.3).

506 The functional MRI data is corrected for distortion (gradient nonlinearity and B0-
507 inhomogeneity) and motion. The distortion from B0 static field inhomogeneity is corrected by
508 means of opposite phase encoding spin echo fieldmap data using TOPUP (Andersson et al.,
509 2003); it is then warped and resampled to MNI space at a 2 mm resolution and saved as a volume

510 in the Neuroimaging Informatics Technology Initiative (NIFTI) format. The region of the
511 cortical ribbon in the fMRI volume is further mapped onto the cortical surface and combined
512 with voxels in the subcortical gray region to create 32k greyordinates in the Connectivity
513 Informatics Technology Initiative (CIFTI) format. Multiple runs of the fMRI data are merged
514 and fed into independent component analyses (ICA) followed by an automated classification of
515 noise components and the removal of noise components using FIX (Salimi-Khorshidi et al.,
516 2014) (Glasser et al., 2018). The automated classifier is trained using the data in this project and
517 its accuracy is maximized. The denoised fMRI data, in combination with other cortical metrics
518 (myelin, thickness; Figure 3B and 3C, respectively), is further used for multi-modal registrations
519 (MSMAll) over the cortical surface, followed by 'de-drifting' (removing registration bias after
520 multimodal registration) based on the group sampled in this study (Glasser et al., 2016a). The
521 resting-state seed-based functional connectivity in an example of a single subject (ID = 9503)
522 revealed a typical pattern over the cerebral cortex across scanners/sites; the left frontal eye field
523 (FEF)-seed functional connectivity showed symmetric coactivation in the bilateral premotor eye
524 field (PEF) (Figure 6A), whereas the left area 55b-seed FC showed an asymmetric language
525 network distributed in the peri-sylvian language (PSL) area, superior temporal sulcus (STS), and
526 areas 44/45 predominantly in the left hemisphere (Figure 6B).
527 The diffusion MRI is corrected for distortion and motion due to gradient nonlinearity,
528 eddy current, motion, and B0 static field inhomogeneity using EDDY (Andersson and
529 Sotiropoulos, 2016). The signal dropouts, susceptibility artefact, and their interaction with
530 motion were also corrected (Andersson et al., 2018; Andersson et al., 2017). The resulting
531 diffusion volumes are merged into a single volume and resampled in the subject's real physical
532 space aligned according to the ACPC convention. Diffusion modeling is performed using nerite

533 orientation density imaging (NODDI) (Fukutomi et al., 2018; Zhang et al., 2012), and a Bayesian

534 estimation of crossing fibers (Behrens et al., 2003; Sotiropoulos et al., 2016). Diffusion

535 probabilistic tractography (Behrens et al., 2003) is also performed in a surface-based analysis

536 (Donahue et al., 2016).

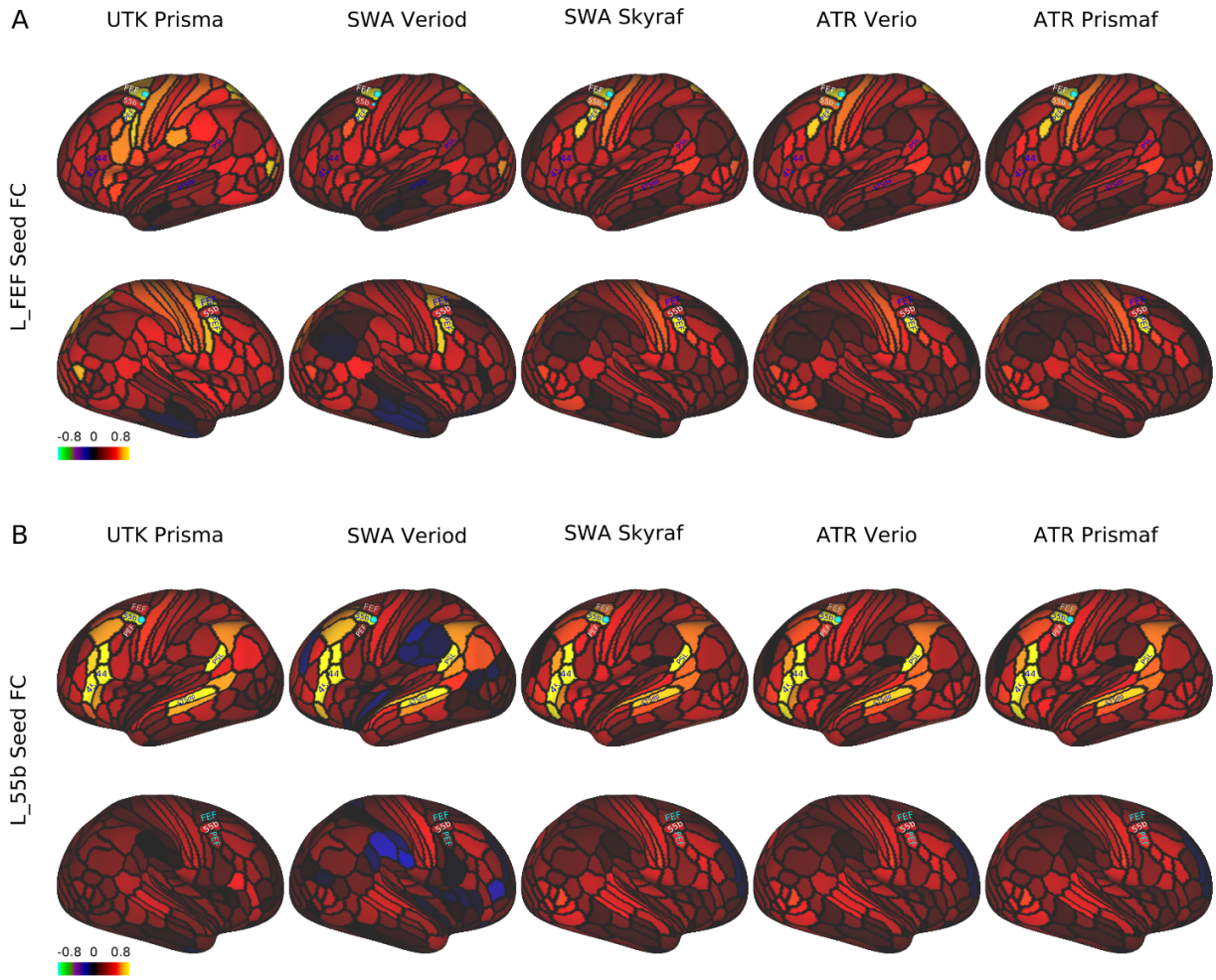

Figure 6. Seed-based resting-state functional connectivity in a single traveling subject across scanners/sites

In a single subject (ID = 9503), the resting-state fMRI scans (5 min x 4) were collected using a scanning protocol of HARP across different scanners/sites (see Supplementary Table S1), preprocessed, and denoised by a surface-based analysis to generate parcellated functional connectivity (FC) using the HCP MMP v1.0 (Glasser et al., 2016a). A) FC seeded from the left frontal eye field (FEF), which was distributed symmetrically in the bilateral premotor eye field (PEF) and comparable across scanners/sites. B) FC seeded from the left area 55b, which showed an asymmetric language network predominant in the left hemisphere that was comparable across

scanners/sites. The language network is distributed in the areas of 44/45, superior temporal sulcus, dorsal posterior part (STSdp), and peri-sylvian language (PSL). Data at https://balsa.wustl.edu/1B9VG and https://balsa.wustl.edu/5Xr71

2.5.3 Preliminary travelling subject data

Here, we show the preliminary results obtained from the initial TS data (as detailed in section 2.4). In the initial TS study (N=30), four healthy subjects participated and travelled across five sites and received MRI scanning with HARP in different scanners (4TS×5S), and twenty six subjects completed test-retest scans in any of 5 scanners (26TS×2/5S). Datasets were analyzed with the current version of preprocessing (see section 2.5.2) and each of the cortical thickness, myelin (non BC), and functional connectivity was parcellated using HCP MMP v1.0 (Glasser et al., 2016a) as described above (a part of the parcellated data in an exemplar subject [ID = 9503] was already shown in Figure 3 and 6). To investigate similarity of the data, each of the parcellated metrics was fed into an analysis of Spearman's rank correlation across subjects and sites/scanners. Figure 7 shows the resultant similarity matrices which demonstrate higher correlation coefficients of within-subjects & between scanners than those of cross-subjects & between scanners in all the metrics of cortical thickness, myelin, and functional connectivity.

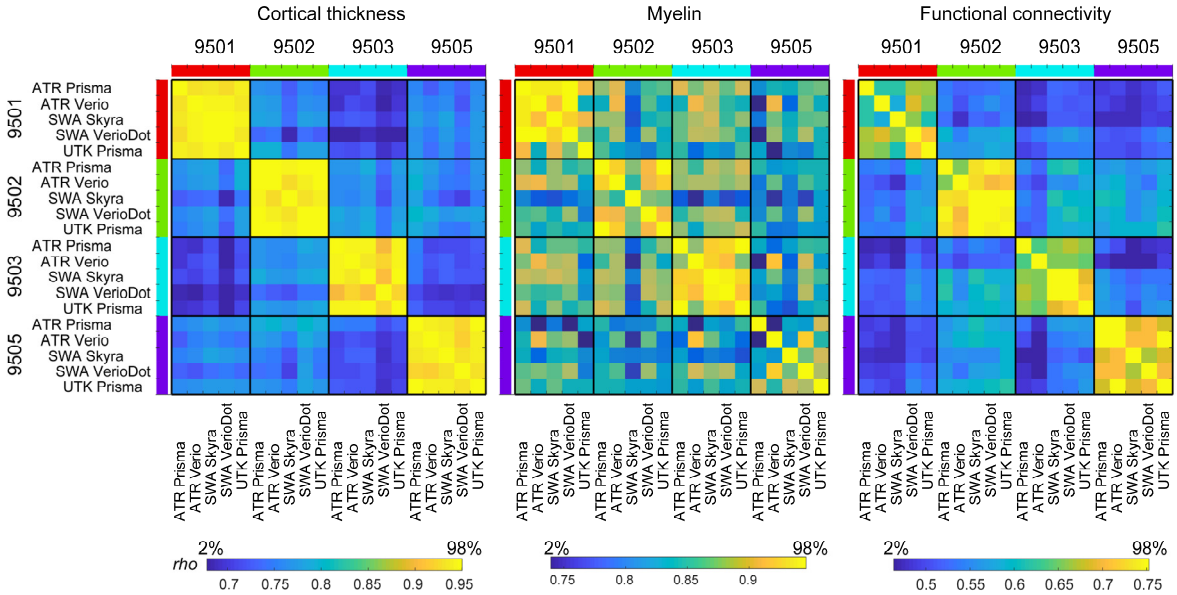

Figure 7. Similarity of the cortical metrics across subjects and sites/scanners in preliminary travelling subject study
From left to right show the correlation matrices of the parcellated cortical thickness, myelin (non BC) and functional connectivity in four travelling subjects (TS). Number of parcellated metrics used for analysis were 360 for thickness and myelin and 129,240 for functional connectivity, which cover all the cerebral cortex in both hemispheres. The correlation coefficient of Spearman's rho is presented by a color bar placed at the bottom.

We also analyzed a different set of TS (N=26), who received test-retest scanning with the HARP protocol in the same MRI sites/scanners. The results (Fig. 8) showed greater similarity of cortical thickness, myelin map, and functional connectivity between test-retest data within subjects as compared with those with different subjects and/or scanners. The correlation coefficients of within-subject & within-scanner were again moderately high and comparable with those of within-subject & between-scanners in Fig 7.

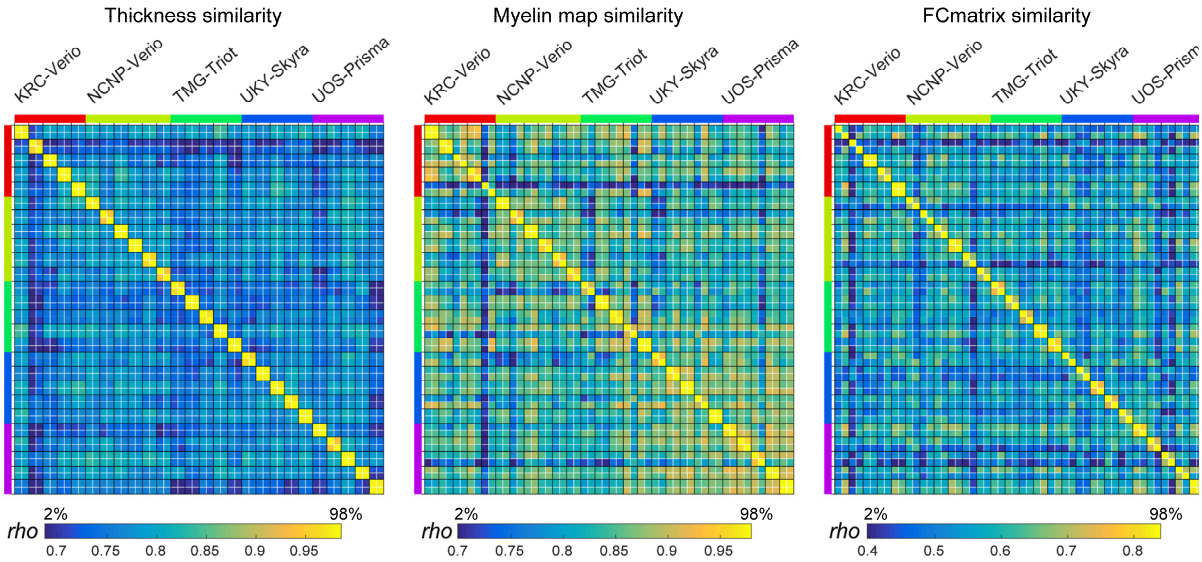

Figure 8. Test-retest results of cortical thickness, myelin (non BC) and resting-state functional connectivity (FC). Note that correlation adjacent to the diagonal and within each black box indicates a single subject's test-retest correlation and is excellent in structure (thickness and myelin) and fairly good in FC. The different sites are colored along the left and top edges.

Table 4 summarizes the similarity values of all the TS30 data in Fig 7 and 8, classified into four types: within-subject & within-scanner, within-subject & between-scanner, between-subject & within-scanner, and between-subject & between-scanner. It is notable that the within-subject similarities are apparently higher than those of between-subject, indicating high sensitivity and reproducibility of subject-wise connectome. The between-subject similarities are smaller than within-subject and almost same across scanners, suggesting minimal bias between scanners and protocols. The within-subject & between-scanner similarity of the myelin map (0.89±0.05) was slightly degraded as compared with within-subject & within-scanner (0.95±0.03), suggesting the residual bias from transmit field across scans, for which we need to develop the correction method in future. That said, these preliminary datasets indicate that the HARP protocols and cortical parcellated analysis provide highly reproducible and specific pattern of subject-wise

connectome, which may effectively enhance statistical harmonization (see Section 2.4) once the data was fully collected in this project.

Table 4. Summary of similarity of cortical measures in TS30

Type of correlation	Thickness	Myelin Map (non BC)	FC matrix
Within-subject & within-scanner correlation (Subject N=26, combination N=26)	0.97 (0.01)	0.95 (0.03)	0.72 (0.08)
Within-subject & between-scanner correlation (Subject N=4, combination N=40)	0.94 (0.01)	0.89 (0.05)	0.69 (0.04)
Between-subject & within-scanner correlation (Subject N=30, combination N=250)	0.76 (0.03)	0.85 (0.05)	0.55 (0.07)
Between-subject & between-scanner correlation (Subject N = 30, combination N=1200)	0.76 (0.03)	0.83 (0.05)	0.55 (0.07)

The values are shown in mean (s.d.). The combination N: a total number of similarity values used for statistics in the matrices in Fig 7 and 8. No BC: non biasfield corrected.

2.5.4. Quality control

QC is implemented in several stages: 1) a brief image check during each scan; 2) an anomaly and abnormality inspection by the radiologists; 3) an assessment of raw data image quality when uploading data to the XNAT server; and 4) preprocessed image quality checks. QC 1 is conducted by site personnel and the participants are rescanned within the same session if scan time remains, if the images have major artifacts, such as those due to head movement. QC 2 is conducted by radiologists at the measurement site or other sites if any radiologist at the site is unable to check the images. QC 3 is manually conducted by researchers at the measurement sites before uploading the data to a server for all images in reference to the HCP QC manual (Marcus et al., 2013). After uploading the images to the XNAT servers, all images are first checked according to the DICOM file information as to whether the images are correctly updated. The researchers at each site are informed of missing DICOM files and any irregular parameters

588 detected in the DICOM files. In QC 3, the T1w and T2w images are manually checked as to
589 whether the face images are completely removed. Then, signal distributions of the myelin map
590 are checked for outliers because of its sensitivity to several artifacts and errors such as motion,
591 reconstruction of the images, and cortical surface reconstruction. Functional and diffusion
592 images are automatically checked for outliers, and the images and data will be checked by visual
593 inspection. In the QC 3 process, a QC pipeline will be implemented for checking the images
594 (Marcus et al., 2013). QC 4 uses preprocessed CIFTI images that will be checked in several
595 preprocessing steps. Any irregular scans and remarks are recorded in the clinical data servers and
596 the information will be used when determining the eligibility criteria for each study.
597
598 *2.6. Ethical regulation*
599 Sharing neuropsychiatric patient data, which may contain information linked to subjects'
600 privacy, requires special attention (Sadato et al., 2019). Therefore, the Brain/MINDS Beyond
601 project put NCNP as the core site for supporting ethical considerations. Before participating in
602 the project, all institutions are required to receive approval from their ethical review board
603 regarding their research plans. This includes the following points and ethical documentation: 1)
604 MR images and clinical data of the participants may be shared within the Brain/MINDS Beyond
605 project or Japanese/International scientific institutions for collaboration. De-identified MR
606 images with limited clinical data (see below) may become publicly accessible on an open
607 database for research purposes. 2) MR images of the participants may be compared with non-
608 human primate MRI data. 3) Intellectual property rights originating from the research of the
609 Brain/MINDS Beyond project shall be attributed to the institutes of the researchers and not the

610 participants. All participants must provide written informed consent to participate in this project
611 after receiving a complete explanation of the experiment.
612 The Japanese regulations for the sharing of personal information used for research
613 purposes requires attention in dealing with two types of data: “individual identification codes”
614 and “special care-required personal information”
615 (http://www.japaneselawtranslation.go.jp/law/detail/?id=2781&vm=04&re=01). Individual
616 identification codes are direct identifiers—information sufficient to identify a specific individual.
617 Special care-required personal information represents indirect identifiers needing special care in
618 handling so as not to cause potential disadvantages to participants. In consideration of these
619 regulations, data accompanied with the MR images are limited in the publicly accessible open
620 database, and only include 5-year age bins, sex, diagnostic information, handedness, simple
621 socioeconomic status, clinical scale scores, and sleepiness scale scores. In the Brain/MINDS
622 Beyond project, we exclude the datasets of MR images containing facial information from the
623 data in the publicly accessible open database.
624
625 *2.7. Data sharing*
626 In the current provisional plan of sharing the collected data, we have designated three types of
627 data sharing:
628 1) Access via an open database: de-identified MR images and limited clinical data are to become
629 publicly accessible for research purposes after the research period ends. The initial release will
630 be scheduled in 2024. Basic demographic and clinical characteristics such as 5-year age bin, sex,
631 socioeconomic status, (premorbid) estimated intellectual quotient, main diagnosis, representative
632 scale scores for each disease and sleepiness during rsfMRI scan will be shared.

2) Application-based sharing: MR images and the clinical datasets are shared after receiving application approval for data usage by the Brain/MINDS Beyond human brain MRI study working group. Applicants are required to obtain approval of their research plan from the ethical review board of their institution and request the dataset type in the application form. The working group discusses the eligibility of the applicants, as well as the availability of the requested dataset, the ethical consideration in the Brain/MINDS Beyond site(s), and any conflict from other applications. Data is released from the distribution server of the Brain/MINDS Beyond project with limited access.

3) Collaboration-based sharing: This form of sharing is used for individual collaborative studies. A research proposal collaborating with the institute(s) in the Brain/MINDS Beyond project is approved by the ethical review board of the institute(s). Data is shared from the relevant institute(s).

645 **3. Discussion**

646 The Brain/MINDS Beyond human brain MRI study expands upon research from previous multi-
647 site neuroimaging studies in Japan and provides high quality brain images by standardizing
648 multiple MRI scanners and protocols. An unbiased and quantitative assessment of cortical
649 structure and function may be needed for sensitive and specific predictions of any dynamics,
650 perturbations, or disorders of the brain system. Multi-modal cross-disease image datasets are
651 systematically and properly acquired, analyzed, and shared to enable investigation of common
652 and disease-specific features for psychiatric and neurological disorders with a high sensitivity
653 and specificity. A distinct feature of this project is to include a study design with the TS project,
654 which enables harmonizing the multi-site data from lower (i.e. preprocessing) to higher levels
655 (i.e. statistics). The harmonization protocols are available at http://mriportal.umin.jp. The
656 Brain/MINDS Beyond human brain MRI project can provide brain imaging biomarkers that are
657 applicable to therapeutic targets and diagnostic supports.

658 To date, several national projects have applied high-quality multimodal MRI protocols, in
659 addition to a preprocessing pipeline, to a large cohort (e.g., HCP, UK biobank, and ABCD).
660 Unlike these multi-site projects, we plan to investigate brain organization associated with brain
661 disorders that occur throughout the lifespan and to develop imaging biomarkers that can be
662 implemented in clinical trials. To facilitate the collection of a larger number of patients with
663 different brain disorders, multiple clinical research sites are participating in this project and
664 cooperating for standardized data acquisitions. The core of the project began from establishing a
665 standardized protocol (i.e. HARP) based on five 3T MRI scanners, but it will continue to develop
666 a comparable protocol for other types of scanners/vendors. The protocol is designed not only for
667 high-resolution structural MRI and high-quality resting-state fMRI, but also for diffusion MRI

668 and other imaging—including scans for correcting distortions. The preprocessing is performed
669 with a surface-based multi-modal analysis to minimize bias largely generated from the variability
670 in cortical folding across subjects (Coalson et al., 2018; Glasser et al., 2016b). The preliminary
671 data demonstrated high quality MRI images and the fidelity of structural and functional brain
672 organizations across scanners/sites. The signal-to-noise ratio of MRI images was very high
673 across scanners/sites (Figure 3A). The cortical metrics of structure (myelin map, thickness)
674 (Figure 3B-C) were comparable to those previously reported in the literature (Fischl and Dale,
675 2000; Glasser and Van Essen, 2011), as well as the functional connectivity related to eye
676 movements involving FEF and PEF (Figure 6A) (Amiez and Petrides, 2009) and a language
677 network involving left 55b, 44/45, STS, and PSL (Figure 6B) (Glasser et al., 2016a). These
678 findings suggest that a surface-based parcellated analysis may provide useful and reliable metrics
679 concerning cortical structure, function, and connectivity, and may potentially contribute to the
680 establishment of multi-modal imaging biomarkers of brain disorders. The initial trial with 30 TS
681 also demonstrated the highly reproducible and specific pattern of subject-wise connectome
682 across five scanners, suggesting the reliability of our prospective harmonization (e.g. protocols
683 and preprocessing) and promising future retrospective (i.e. statistical) harmonization. The
684 residual bias of myelin map is presumably due to differences of transmit field across scans and
685 needs to be corrected in future preprocessing pipeline.

686 The TS approach is a novel harmonization method for multi-site brain image data
687 (Yamashita et al., 2019), which has proven that measurement bias from MRI equipment and
688 protocols can be differentiated from sampling bias between sites. Instead of using a previously
689 applied GLM, we plan to expand the statistical approach to a GLMM in this project. One of the
690 obstacles of the GLMM approach is that it requires a larger number of total scans compared to

691 those in a GLM approach; overlapping scans at hub sites are required for all TS participants to
692 ensure the data connectivity; additionally, a larger number of TS participants is required in the
693 TS project because the degree of freedom can be reduced in the GLMM. However, one of the
694 benefits of the GLMM approach includes that it is flexible with the variability in data
695 acquisition—such as the number of scans per participant and length of scan time per protocol;
696 thus, is suitable for a big project. Furthermore, this approach allows the addition of another site,
697 scanner, and protocol to an existing TS network, which can deal with the future upgrades of
698 scanners and protocols. In fact, the scanners at two sites (UHI and SWA) were upgraded to a
699 MAGNETOM Skyra fit (Siemens Healthcare GmbH, Erlangen, Germany) for institutional
700 reasons after the Brain/MINDS Beyond project had started. Therefore, we customized the TS for
701 two sites to ensure that the data are properly connected before and after the upgrades. Also, the
702 project welcomes other sites to participate in the TS network.
703 Because this project focuses on various brain disorders across the lifespan, we aim to
704 identify common and disease-specific features of psychiatric and neurological disorders. While
705 some case-control studies suggest possible neural mechanisms in a psychiatric disease, other
706 studies suggest that the effects may not be specific to a single entity but instead may be shared
707 across multiple neuropsychiatric disorders (Hibar et al., 2018; Schmaal et al., 2017; Schmaal et
708 al., 2016; van Erp et al., 2016). Such non-specificity may be at least partly addressed by
709 investigating diseases across the lifespan, since some of brain changes reported in psychiatric
710 disorders also occur in aging or development in healthy subjects, e.g. volumetric changes in
711 subcortical structures in schizophrenia (Okada et al., 2016; van Erp et al., 2016) and in healthy
712 aging (O'Shea et al., 2016; Wang et al., 2019). We initially coordinated with 13 sites to explore
713 various psychiatric and neurological disorders throughout the lifespan and to make use of a

714 powerful harmonization method. Therefore, this project aims to identify both the common and
715 disease-specific pathophysiology features of psychiatric and neurological disorders, which will
716 hopefully lead to imaging biomarkers for general clinical practice and the development of
717 candidate therapeutic targets for future clinical trials.

718 We established task fMRI scans using EMOTION and CARIT in HARP to evaluate the
719 validity, reliability and applicability of harmonization. The result of task fMRI may be used for
720 validation of the resting-state fMRI based cortical surface registration, and parcellation. The TS
721 project performing task fMRI is now under planning and hopefully will be completed in coming
722 years.

723 In conclusion, the Brain/MINDS Beyond human brain MRI project began with the
724 participation of 13 clinical research sites—all of which have setup brain image scans using the
725 standard MRI scanners and protocols, conducted TS scans, and will share acquired data with the
726 project and the public in the future, and commit to the analysis and publication of the data. To
727 the best of our knowledge, this is the first human brain MRI project to explore psychiatric and
728 neurological disorders across the lifespan. The project aims to discover robust findings which
729 may be directly related to the common or disease-specific pathophysiology features of such
730 diseases and facilitate the development of candidate biomarkers for clinical application and drug
731 discovery.

Acknowledgment

This research was supported by the Agency for Medical Research and Development (AMED) under Grant Numbers JP20dm0307001 (K.K.), JP20dm0307002 (Y.O.), JP20dm0307003 (T.Han.), JP20dm0307004 (K.K.), JP20dm0307008 (M.K.), JP20dm`0307020 (N.S.), JP20dm0207069 (S.K.) and JP20dm0307006 (T.Hay.). This study was also supported by the University of Tokyo Center for Integrative Science of Human Behaviour (CiSHuB) and the International Research Center for Neurointelligence (WPI-IRCN) at the University of Tokyo Institutes for Advanced Study (UTIAS).

Author Contributions

Shinsuke Koike, Conceptualization, Project administration, Funding acquisition, Writing – original draft, Software, Resources.

Saori C Tanaka, Conceptualization, Project administration, Data Curation, Software, Resources, Writing – original draft.

Tomohisa Okada, Methodology, Investigation.

Toshihiko Aso, Investigation, Formal Analysis, Validation.

Michiko Asano, Investigation, Data curation.

Norihide Maikusa, Methodology, Resources.

Kentaro Morita, Writing – original draft.

Naohiro Okada, Investigation, Writing – original draft.

Masaki Fukunaga, Methodology.

Akiko Uematsu, Methodology, Investigation.

Hiroki Togo, Methodology, Investigation.

Atsushi Miyazaki, Methodology, Investigation.

Katsutoshi Murata, Methodology.

Yuta Urushibata, Methodology.

Joonas Autio, Methodology.

Takayuki Ose, Methodology.

Junichiro Yoshimoto, Methodology.

Toshiyuki Araki, Writing – original draft.

Matthew F Glasser, Software, Writing - reviewing and editing.

David C Van Essen, Writing – reviewing and editing.

Megumi Maruyma, Project administration.

Norihiro Sadato, Investigation, Funding acquisition, Project administration.

Mitsuo Kawato, Conceptualization, Funding acquisition, Project administration.

Kiyoto Kasai, Investigation, Funding acquisition, Project administration, Supervision.

Yasumasa Okamoto, Investigation, Funding acquisition.

Takashi Hanakawa, Project administration, Funding Acquisition, Methodology, Investigation, Resources, Writing – original draft.

Takuya Hayashi, Conceptualization, Project administration, Funding Acquisition, Software, Resources, Formal Analysis, Writing - original draft, reviewing and editing.

Conflict of interest

Katsutoshi Murata and Yuta Urushibara are employed by Siemens Healthcare K.K., Tokyo, Japan. The other authors report no financial relationships with commercial interests.

Data availability

The data presented in Figure 3 and 6 are available at BALSA (https://balsa.wustl.edu/study/show/npD26). Harmonization protocols and other information of the project are available at the BrainMINDS beyond MRI portal site (http://mriportal.umin.jp/?lang=en). The tool for DICOM to NIFTI conversion, folder structure, derivation of imaging parameters is available at https://github.com/RIKEN-BCIL/BCILDCMCONVERT, See also Data sharing section in details of data obtained in future in this project. For proposal and requests for the data usage, please contact to Saori Tanaka (xsaori@atr.jp).

References

Amiez, C., Petrides, M., 2009. Anatomical organization of the eye fields in the human and non-human primate frontal cortex. Prog Neurobiol 89, 220-230.

Andersson, J.L., Skare, S., Ashburner, J., 2003. How to correct susceptibility distortions in spin-echo echo-planar images: application to diffusion tensor imaging. Neuroimage 20, 870-888.

Andersson, J.L.R., Graham, M.S., Drobnjak, I., Zhang, H., Campbell, J., 2018. Susceptibility-induced distortion that varies due to motion: Correction in diffusion MR without acquiring additional data. Neuroimage 171, 277-295.

Andersson, J.L.R., Graham, M.S., Drobnjak, I., Zhang, H., Filippini, N., Bastiani, M., 2017. Towards a comprehensive framework for movement and distortion correction of diffusion MR images: Within volume movement. Neuroimage 152, 450-466.

Andersson, J.L.R., Sotiropoulos, S.N., 2016. An integrated approach to correction for off-resonance effects and subject movement in diffusion MR imaging. Neuroimage 125, 1063-1078.

Ando, S., Nishida, A., Yamasaki, S., Koike, S., Morimoto, Y., Hoshino, A., Kanata, S., Fujikawa, S., Endo, K., Usami, S., Furukawa, T.A., Hiraiwa-Hasegawa, M., Kasai, K., Scientific, T.T.C., Data Collection, T., 2019. Cohort Profile: The Tokyo Teen Cohort study (TTC). Int J Epidemiol 48, 1414-1414g.

Beheshti, I., Maikusa, N., Daneshmand, M., Matsuda, H., Demirel, H., Anbarjafari, G., Japanese-Alzheimer's Disease Neuroimaging, I., 2017. Classification of Alzheimer's Disease and Prediction of Mild Cognitive Impairment Conversion Using Histogram-Based Analysis of Patient-Specific Anatomical Brain Connectivity Networks. J Alzheimers Dis 60, 295-304.

Behrens, T.E., Woolrich, M.W., Jenkinson, M., Johansen-Berg, H., Nunes, R.G., Clare, S., Matthews, P.M., Brady, J.M., Smith, S.M., 2003. Characterization and propagation of uncertainty in diffusion-weighted MR imaging. Magn Reson Med 50, 1077-1088.

Bookheimer, S.Y., Salat, D.H., Terpstra, M., Ances, B.M., Barch, D.M., Buckner, R.L., Burgess, G.C., Curtiss, S.W., Diaz-Santos, M., Elam, J.S., Fischl, B., Greve, D.N., Hagy, H.A., Harms, M.P., Hatch, O.M., Hedden, T., Hodge, C., Japardi, K.C., Kuhn, T.P., Ly, T.K., Smith, S.M., Somerville, L.H., Ugurbil, K., van der Kouwe, A., Van Essen, D., Woods, R.P., Yacoub, E., 2019. The Lifespan Human Connectome Project in Aging: An overview. Neuroimage 185, 335-348.

Casey, B.J., Cannonier, T., Conley, M.I., Cohen, A.O., Barch, D.M., Heitzeg, M.M., Soules, M.E., Teslovich, T., Dellarco, D.V., Garavan, H., Orr, C.A., Wager, T.D., Banich, M.T., Speer, N.K., Sutherland, M.T., Riedel, M.C., Dick, A.S., Bjork, J.M., Thomas, K.M., Chaarani, B., Mejia, M.H., Hagler, D.J., Jr., Daniela Cornejo, M., Sicat, C.S., Harms, M.P., Dosenbach, N.U.F., Rosenberg, M., Earl, E., Bartsch, H., Watts, R., Polimeni, J.R., Kuperman, J.M., Fair, D.A., Dale, A.M., Workgroup, A.I.A., 2018. The Adolescent Brain Cognitive Development (ABCD) study: Imaging acquisition across 21 sites. Dev Cogn Neurosci 32, 43-54.

Coalson, T.S., Van Essen, D.C., Glasser, M.F., 2018. The impact of traditional neuroimaging methods on the spatial localization of cortical areas. Proc Natl Acad Sci U S A 115, E6356-E6365.

Degenhardt, L., Chiu, W.T., Sampson, N., Kessler, R.C., Anthony, J.C., Angermeyer, M., Bruffaerts, R., de Girolamo, G., Gureje, O., Huang, Y., Karam, A., Kostyuchenko, S., Lepine, J.P., Mora, M.E., Neumark, Y., Ormel, J.H., Pinto-Meza, A., Posada-Villa, J., Stein, D.J., Takeshima, T., Wells, J.E., 2008. Toward a global view of alcohol, tobacco, cannabis, and cocaine use: findings from the WHO World Mental Health Surveys. PLoS Med 5, e141.

Donahue, C.J., Sotiropoulos, S.N., Jbabdi, S., Hernandez-Fernandez, M., Behrens, T.E., Dyrby, T.B., Coalson, T., Kennedy, H., Knoblauch, K., Van Essen, D.C., Glasser, M.F., 2016. Using Diffusion Tractography to Predict Cortical Connection Strength and Distance: A Quantitative Comparison with Tracers in the Monkey. J Neurosci 36, 6758-6770.

Drysdale, A.T., Grosenick, L., Downar, J., Dunlop, K., Mansouri, F., Meng, Y., Fetcho, R.N., Zebley, B., Oathes, D.J., Etkin, A., Schatzberg, A.F., Sudheimer, K., Keller, J., Mayberg, H.S., Gunning, F.M., Alexopoulos, G.S., Fox, M.D., Pascual-Leone, A., Voss, H.U., Casey, B.J., Dubin, M.J., Liston, C.,

2017. Resting-state connectivity biomarkers define neurophysiological subtypes of depression. Nat Med 23, 28-38.
Elliott, L.T., Sharp, K., Alfaro-Almagro, F., Shi, S., Miller, K.L., Douaud, G., Marchini, J., Smith, S.M., 2018a. Genome-wide association studies of brain imaging phenotypes in UK Biobank. Nature 562, 210-216.
Elliott, M.L., Romer, A., Knodt, A.R., Hariri, A.R., 2018b. A Connectome-wide Functional Signature of Transdiagnostic Risk for Mental Illness. Biol Psychiatry 84, 452-459.
Fischl, B., 2012. FreeSurfer. Neuroimage 62, 774-781.
Fischl, B., Dale, A.M., 2000. Measuring the thickness of the human cerebral cortex from magnetic resonance images. Proc Natl Acad Sci U S A 97, 11050-11055.
Fortin, J.P., Cullen, N., Sheline, Y.I., Taylor, W.D., Aselcioglu, I., Cook, P.A., Adams, P., Cooper, C., Fava, M., McGrath, P.J., McInnis, M., Phillips, M.L., Trivedi, M.H., Weissman, M.M., Shinohara, R.T., 2018. Harmonization of cortical thickness measurements across scanners and sites. Neuroimage 167, 104-120.
Fortin, J.P., Parker, D., Tunc, B., Watanabe, T., Elliott, M.A., Ruparel, K., Roalf, D.R., Satterthwaite, T.D., Gur, R.C., Gur, R.E., Schultz, R.T., Verma, R., Shinohara, R.T., 2017. Harmonization of multi-site diffusion tensor imaging data. Neuroimage 161, 149-170.
Fukutomi, H., Glasser, M.F., Zhang, H., Autio, J.A., Coalson, T.S., Okada, T., Togashi, K., Van Essen, D.C., Hayashi, T., 2018. Neurite imaging reveals microstructural variations in human cerebral cortical gray matter. Neuroimage 182, 488-499.
Glasser, M.F., Coalson, T.S., Robinson, E.C., Hacker, C.D., Harwell, J., Yacoub, E., Ugurbil, K., Andersson, J., Beckmann, C.F., Jenkinson, M., Smith, S.M., Van Essen, D.C., 2016a. A multi-modal parcellation of human cerebral cortex. Nature 536, 171-178.
Glasser, M.F., Smith, S.M., Marcus, D.S., Andersson, J.L., Auerbach, E.J., Behrens, T.E., Coalson, T.S., Harms, M.P., Jenkinson, M., Moeller, S., Robinson, E.C., Sotiropoulos, S.N., Xu, J., Yacoub, E., Ugurbil, K., Van Essen, D.C., 2016b. The Human Connectome Project's neuroimaging approach. Nat Neurosci 19, 1175-1187.
Glasser, M.F., Sotiropoulos, S.N., Wilson, J.A., Coalson, T.S., Fischl, B., Andersson, J.L., Xu, J., Jbabdi, S., Webster, M., Polimeni, J.R., Van Essen, D.C., Jenkinson, M., Consortium, W.U.-M.H., 2013. The minimal preprocessing pipelines for the Human Connectome Project. Neuroimage 80, 105-124.
Glasser, M.F., Van Essen, D.C., 2011. Mapping human cortical areas in vivo based on myelin content as revealed by T1- and T2-weighted MRI. J Neurosci 31, 11597-11616.
Harms, M.P., Somerville, L.H., Ances, B.M., Andersson, J., Barch, D.M., Bastiani, M., Bookheimer, S.Y., Brown, T.B., Buckner, R.L., Burgess, G.C., Coalson, T.S., Chappell, M.A., Dapretto, M., Douaud, G., Fischl, B., Glasser, M.F., Greve, D.N., Hodge, C., Jamison, K.W., Jbabdi, S., Kandala, S., Li, X., Mair, R.W., Mangia, S., Marcus, D., Mascali, D., Moeller, S., Nichols, T.E., Robinson, E.C., Salat, D.H., Smith, S.M., Sotiropoulos, S.N., Terpstra, M., Thomas, K.M., Tisdall, M.D., Ugurbil, K., van der Kouwe, A., Woods, R.P., Zollei, L., Van Essen, D.C., Yacoub, E., 2018. Extending the Human Connectome Project across ages: Imaging protocols for the Lifespan Development and Aging projects. Neuroimage 183, 972-984.
Hibar, D.P., Westlye, L.T., Doan, N.T., Jahanshad, N., Cheung, J.W., Ching, C.R.K., Versace, A., Bilderbeck, A.C., Uhlmann, A., Mwangi, B., Kramer, B., Overs, B., Hartberg, C.B., Abe, C., Dima, D., Grotegerd, D., Sprooten, E., Boen, E., Jimenez, E., Howells, F.M., Delvecchio, G., Temmingh, H., Starke, J., Almeida, J.R.C., Goikolea, J.M., Houenou, J., Beard, L.M., Rauer, L., Abramovic, L., Bonnin, M., Ponteduro, M.F., Keil, M., Rive, M.M., Yao, N., Yalin, N., Najt, P., Rosa, P.G., Redlich, R., Trost, S., Hagenaars, S., Fears, S.C., Alonso-Lana, S., van Erp, T.G.M., Nickson, T., Chaim-Avancini, T.M., Meier, T.B., Elvsashagen, T., Haukvik, U.K., Lee, W.H., Schene, A.H., Lloyd, A.J., Young, A.H., Nugent, A., Dale, A.M., Pfennig, A., McIntosh, A.M., Lafer, B., Baune, B.T., Ekman, C.J., Zarate, C.A., Bearden, C.E., Henry, C., Simhandl, C., McDonald, C., Bourne, C., Stein, D.J., Wolf, D.H., Cannon, D.M., Glahn, D.C., Veltman, D.J., Pomarol-Clotet, E., Vieta, E., Canales-Rodriguez, E.J., Nery, F.G., Duran, F.L.S., Busatto, G.F., Roberts, G., Pearlson, G.D., Goodwin,

G.M., Kugel, H., Whalley, H.C., Ruhe, H.G., Soares, J.C., Fullerton, J.M., Rybakowski, J.K., Savitz, J., Chaim, K.T., Fatjo-Vilas, M., Soeiro-de-Souza, M.G., Boks, M.P., Zanetti, M.V., Otaduy, M.C.G., Schaufelberger, M.S., Alda, M., Ingvar, M., Phillips, M.L., Kempton, M.J., Bauer, M., Landen, M., Lawrence, N.S., van Haren, N.E.M., Horn, N.R., Freimer, N.B., Gruber, O., Schofield, P.R., Mitchell, P.B., Kahn, R.S., Lenroot, R., Machado-Vieira, R., Ophoff, R.A., Sarro, S., Frangou, S., Satterthwaite, T.D., Hajek, T., Dannlowski, U., Malt, U.F., Arolt, V., Gattaz, W.F., Drevets, W.C., Caseras, X., Agartz, I., Thompson, P.M., Andreassen, O.A., 2018. Cortical abnormalities in bipolar disorder: an MRI analysis of 6503 individuals from the ENIGMA Bipolar Disorder Working Group. Mol Psychiatry 23, 932-942.

Iwatsubo, T., Iwata, A., Suzuki, K., Ihara, R., Arai, H., Ishii, K., Senda, M., Ito, K., Ikeuchi, T., Kuwano, R., Matsuda, H., Japanese Alzheimer's Disease Neuroimaging, I., Sun, C.K., Beckett, L.A., Petersen, R.C., Weiner, M.W., Aisen, P.S., Donohue, M.C., Alzheimer's Disease Neuroimaging, I., 2018. Japanese and North American Alzheimer's Disease Neuroimaging Initiative studies: Harmonization for international trials. Alzheimers Dement 14, 1077-1087.

Koike, S., Takano, Y., Iwashiro, N., Satomura, Y., Suga, M., Nagai, T., Natsubori, T., Tada, M., Nishimura, Y., Yamasaki, S., Takizawa, R., Yahata, N., Araki, T., Yamasue, H., Kasai, K., 2013. A multimodal approach to investigate biomarkers for psychosis in a clinical setting: the Integrative Neuroimaging studies in Schizophrenia Targeting for Early intervention and Prevention (IN-STEP) project Schizophr Res 143, 116-124.

Koutsouleris, N., Meisenzahl, E.M., Borgwardt, S., Riecher-Rossler, A., Frodl, T., Kambeitz, J., Kohler, Y., Falkai, P., Moller, H.J., Reiser, M., Davatzikos, C., 2015. Individualized differential diagnosis of schizophrenia and mood disorders using neuroanatomical biomarkers. Brain 138, 2059-2073.

Lee, T.Y., Kwon, J.S., 2016. Psychosis research in Asia: advantage from low prevalence of cannabis use. NPJ Schizophr 2, 1.

Marcus, D.S., Harms, M.P., Snyder, A.Z., Jenkinson, M., Wilson, J.A., Glasser, M.F., Barch, D.M., Archie, K.A., Burgess, G.C., Ramaratnam, M., Hodge, M., Horton, W., Herrick, R., Olsen, T., McKay, M., House, M., Hileman, M., Reid, E., Harwell, J., Coalson, T., Schindler, J., Elam, J.S., Curtiss, S.W., Van Essen, D.C., Consortium, W.U.-M.H., 2013. Human Connectome Project informatics: quality control, database services, and data visualization. Neuroimage 80, 202-219.

Miller, K.L., Alfaro-Almagro, F., Bangerter, N.K., Thomas, D.L., Yacoub, E., Xu, J., Bartsch, A.J., Jbabdi, S., Sotiropoulos, S.N., Andersson, J.L., Griffanti, L., Douaud, G., Okell, T.W., Weale, P., Dragonu, I., Garratt, S., Hudson, S., Collins, R., Jenkinson, M., Matthews, P.M., Smith, S.M., 2016. Multimodal population brain imaging in the UK Biobank prospective epidemiological study. Nat Neurosci 19, 1523-1536.

Moeller, S., Yacoub, E., Olman, C.A., Auerbach, E., Strupp, J., Harel, N., Ugurbil, K., 2010. Multiband multislice GE-EPI at 7 tesla, with 16-fold acceleration using partial parallel imaging with application to high spatial and temporal whole-brain fMRI. Magn Reson Med 63, 1144-1153.

Mueller, S.G., Weiner, M.W., Thal, L.J., Petersen, R.C., Jack, C., Jagust, W., Trojanowski, J.Q., Toga, A.W., Beckett, L., 2005. The Alzheimer's disease neuroimaging initiative. Neuroimaging Clin N Am 15, 869-877, xi-xii.

Mukai, Y., Murata, M., 2017. Japan Parkinson's Progression Markers Initiative (J-PPMI). Nihon Rinsho 75, 151-155.

Murray, C.J., Vos, T., Lozano, R., Naghavi, M., Flaxman, A.D., Michaud, C., Ezzati, M., Shibuya, K., Salomon, J.A., Abdalla, S., Aboyans, V., Abraham, J., Ackerman, I., Aggarwal, R., Ahn, S.Y., Ali, M.K., Alvarado, M., Anderson, H.R., Anderson, L.M., Andrews, K.G., Atkinson, C., Baddour, L.M., Bahalim, A.N., Barker-Collo, S., Barrero, L.H., Bartels, D.H., Basanez, M.G., Baxter, A., Bell, M.L., Benjamin, E.J., Bennett, D., Bernabe, E., Bhalla, K., Bhandari, B., Bikbov, B., Bin Abdulhak, A., Birbeck, G., Black, J.A., Blencowe, H., Blore, J.D., Blyth, F., Bolliger, I., Bonaventure, A., Boufous, S., Bourne, R., Boussinesq, M., Braithwaite, T., Brayne, C., Bridgett, L., Brooker, S., Brooks, P., Brugha, T.S., Bryan-Hancock, C., Bucello, C., Buchbinder, R., Buckle, G., Budke, C.M., Burch, M., Burney, P., Burstein, R., Calabria, B., Campbell, B., Canter, C.E., Carabin, H., Carapetis, J.,

Carmona, L., Cella, C., Charlson, F., Chen, H., Cheng, A.T., Chou, D., Chugh, S.S., Coffeng, L.E., Colan, S.D., Colquhoun, S., Colson, K.E., Condon, J., Connor, M.D., Cooper, L.T., Corriere, M., Cortinovis, M., de Vaccaro, K.C., Couser, W., Cowie, B.C., Criqui, M.H., Cross, M., Dabhadkar, K.C., Dahiya, M., Dahodwala, N., Damsere-Derry, J., Danaei, G., Davis, A., De Leo, D., Degenhardt, L., Dellavalle, R., Delossantos, A., Denenberg, J., Derrett, S., Des Jarlais, D.C., Dharmaratne, S.D., Dherani, M., Diaz-Torne, C., Dolk, H., Dorsey, E.R., Driscoll, T., Duber, H., Ebel, B., Edmond, K., Elbaz, A., Ali, S.E., Erskine, H., Erwin, P.J., Espindola, P., Ewoigbokhan, S.E., Farzadfar, F., Feigin, V., Felson, D.T., Ferrari, A., Ferri, C.P., Fevre, E.M., Finucane, M.M., Flaxman, S., Flood, L., Foreman, K., Forouzanfar, M.H., Fowkes, F.G., Fransen, M., Freeman, M.K., Gabbe, B.J., Gabriel, S.E., Gakidou, E., Ganatra, H.A., Garcia, B., Gaspari, F., Gillum, R.F., Gmel, G., Gonzalez-Medina, D., Gosselin, R., Grainger, R., Grant, B., Groeger, J., Guillemin, F., Gunnell, D., Gupta, R., Haagsma, J., Hagan, H., Halasa, Y.A., Hall, W., Haring, D., Haro, J.M., Harrison, J.E., Havmoeller, R., Hay, R.J., Higashi, H., Hill, C., Hoen, B., Hoffman, H., Hotez, P.J., Hoy, D., Huang, J.J., Ibeanusi, S.E., Jacobsen, K.H., James, S.L., Jarvis, D., Jasrasaria, R., Jayaraman, S., Johns, N., Jonas, J.B., Karthikeyan, G., Kassebaum, N., Kawakami, N., Keren, A., Khoo, J.P., King, C.H., Knowlton, L.M., Kobusingye, O., Koranteng, A., Krishnamurthi, R., Laden, F., Lalloo, R., Laslett, L.L., Lathlean, T., Leasher, J.L., Lee, Y.Y., Leigh, J., Levinson, D., Lim, S.S., Limb, E., Lin, J.K., Lipnick, M., Lipshultz, S.E., Liu, W., Loane, M., Ohno, S.L., Lyons, R., Mabweijano, J., MacIntyre, M.F., Malekzadeh, R., Mallinger, L., Manivannan, S., Marcenes, W., March, L., Margolis, D.J., Marks, G.B., Marks, R., Matsumori, A., Matzopoulos, R., Mayosi, B.M., McAnulty, J.H., McDermott, M.M., McGill, N., McGrath, J., Medina-Mora, M.E., Meltzer, M., Mensah, G.A., Merriman, T.R., Meyer, A.C., Miglioli, V., Miller, M., Miller, T.R., Mitchell, P.B., Mock, C., Mocumbi, A.O., Moffitt, T.E., Mokdad, A.A., Monasta, L., Montico, M., Moradi-Lakeh, M., Moran, A., Morawska, L., Mori, R., Murdoch, M.E., Mwaniki, M.K., Naidoo, K., Nair, M.N., Naldi, L., Narayan, K.M., Nelson, P.K., Nelson, R.G., Nevitt, M.C., Newton, C.R., Nolte, S., Norman, P., Norman, R., O'Donnell, M., O'Hanlon, S., Olives, C., Omer, S.B., Ortblad, K., Osborne, R., Ozgediz, D., Page, A., Pahari, B., Pandian, J.D., Rivero, A.P., Patten, S.B., Pearce, N., Padilla, R.P., Perez-Ruiz, F., Perico, N., Pesudovs, K., Phillips, D., Phillips, M.R., Pierce, K., Pion, S., Polanczyk, G.V., Polinder, S., Pope, C.A., 3rd, Popova, S., Porrini, E., Pourmalek, F., Prince, M., Pullan, R.L., Ramaiah, K.D., Ranganathan, D., Razavi, H., Regan, M., Rehm, J.T., Rein, D.B., Remuzzi, G., Richardson, K., Rivara, F.P., Roberts, T., Robinson, C., De Leon, F.R., Ronfani, L., Room, R., Rosenfeld, L.C., Rushton, L., Sacco, R.L., Saha, S., Sampson, U., Sanchez-Riera, L., Sanman, E., Schwebel, D.C., Scott, J.G., Segui-Gomez, M., Shahraz, S., Shepard, D.S., Shin, H., Shivakoti, R., Singh, D., Singh, G.M., Singh, J.A., Singleton, J., Sleet, D.A., Sliwa, K., Smith, E., Smith, J.L., Stapelberg, N.J., Steer, A., Steiner, T., Stolk, W.A., Stovner, L.J., Sudfeld, C., Syed, S., Tamburlini, G., Tavakkoli, M., Taylor, H.R., Taylor, J.A., Taylor, W.J., Thomas, B., Thomson, W.M., Thurston, G.D., Tleyjeh, I.M., Tonelli, M., Towbin, J.A., Truelsen, T., Tsilimbaris, M.K., Ubeda, C., Undurraga, E.A., van der Werf, M.J., van Os, J., Vavilala, M.S., Venketasubramanian, N., Wang, M., Wang, W., Watt, K., Weatherall, D.J., Weinstock, M.A., Weintraub, R., Weisskopf, M.G., Weissman, M.M., White, R.A., Whiteford, H., Wiebe, N., Wiersma, S.T., Wilkinson, J.D., Williams, H.C., Williams, S.R., Witt, E., Wolfe, F., Woolf, A.D., Wulf, S., Yeh, P.H., Zaidi, A.K., Zheng, Z.J., Zonies, D., Lopez, A.D., AlMazroa, M.A., Memish, Z.A., 2012. Disability-adjusted life years (DALYs) for 291 diseases and injuries in 21 regions, 1990-2010: a systematic analysis for the Global Burden of Disease Study 2010. Lancet 380, 2197-2223.

Nunes, A., Schnack, H.G., Ching, C.R.K., Agartz, I., Akudjedu, T.N., Alda, M., Alnaes, D., Alonso-Lana, S., Bauer, J., Baune, B.T., Boen, E., Bonnin, C.D.M., Busatto, G.F., Canales-Rodriguez, E.J., Cannon, D.M., Caseras, X., Chaim-Avancini, T.M., Dannlowski, U., Diaz-Zuluaga, A.M., Dietsche, B., Doan, N.T., Duchesnay, E., Elvsashagen, T., Emden, D., Eyler, L.T., Fatjo-Vilas, M., Favre, P., Foley, S.F., Fullerton, J.M., Glahn, D.C., Goikolea, J.M., Grotegerd, D., Hahn, T., Henry, C., Hibar, D.P., Houenou, J., Howells, F.M., Jahanshad, N., Kaufmann, T., Kenney, J., Kircher, T.T.J., Krug, A., Lagerberg, T.V., Lenroot, R.K., Lopez-Jaramillo, C., Machado-Vieira, R., Malt, U.F., McDonald,

C., Mitchell, P.B., Mwangi, B., Nabulsi, L., Opel, N., Overs, B.J., Pineda-Zapata, J.A., Pomarol-Clotet, E., Redlich, R., Roberts, G., Rosa, P.G., Salvador, R., Satterthwaite, T.D., Soares, J.C., Stein, D.J., Temmingh, H.S., Trappenberg, T., Uhlmann, A., van Haren, N.E.M., Vieta, E., Westlye, L.T., Wolf, D.H., Yuksel, D., Zanetti, M.V., Andreassen, O.A., Thompson, P.M., Hajek, T., Group, E.B.D.W., 2018. Using structural MRI to identify bipolar disorders - 13 site machine learning study in 3020 individuals from the ENIGMA Bipolar Disorders Working Group. Mol Psychiatry.

O'Shea, A., Cohen, R.A., Porges, E.C., Nissim, N.R., Woods, A.J., 2016. Cognitive Aging and the Hippocampus in Older Adults. Front Aging Neurosci 8, 298.

Okada, N., Ando, S., Sanada, M., Hirata-Mogi, S., Iijima, Y., Sugiyama, H., Shirakawa, T., Yamagishi, M., Kanehara, A., Morita, M., Yagi, T., Hayashi, N., Koshiyama, D., Morita, K., Sawada, K., Ikegame, T., Sugimoto, N., Toriyama, R., Masaoka, M., Fujikawa, S., Kanata, S., Tada, M., Kirihara, K., Yahata, N., Araki, T., Jinde, S., Kano, Y., Koike, S., Endo, K., Yamasaki, S., Nishida, A., Hiraiwa-Hasegawa, M., Bundo, M., Iwamoto, K., Tanaka, S.C., Kasai, K., 2019. Population-neuroscience study of the Tokyo TEEN Cohort (pn-TTC): Cohort longitudinal study to explore the neurobiological substrates of adolescent psychological and behavioral development. Psychiatry Clin Neurosci 73, 231-242.

Okada, N., Fukunaga, M., Yamashita, F., Koshiyama, D., Yamamori, H., Ohi, K., Yasuda, Y., Fujimoto, M., Watanabe, Y., Yahata, N., Nemoto, K., Hibar, D.P., van Erp, T.G., Fujino, H., Isobe, M., Isomura, S., Natsubori, T., Narita, H., Hashimoto, N., Miyata, J., Koike, S., Takahashi, T., Yamasue, H., Matsuo, K., Onitsuka, T., Iidaka, T., Kawasaki, Y., Yoshimura, R., Watanabe, Y., Suzuki, M., Turner, J.A., Takeda, M., Thompson, P.M., Ozaki, N., Kasai, K., Hashimoto, R., 2016. Abnormal asymmetries in subcortical brain volume in schizophrenia. Mol Psychiatry 21, 1460-1466.

Parkinson Progression Marker Initiative, 2011. The Parkinson Progression Marker Initiative (PPMI). Prog Neurobiol 95, 629-635.

R Core Team, 2018. R: A language and environment for statistical computing. R Foundation for Statistical Computing. Vienna, Austria.

Robinson, E.C., Garcia, K., Glasser, M.F., Chen, Z., Coalson, T.S., Makropoulos, A., Bozek, J., Wright, R., Schuh, A., Webster, M., Hutter, J., Price, A., Cordero Grande, L., Hughes, E., Tusor, N., Bayly, P.V., Van Essen, D.C., Smith, S.M., Edwards, A.D., Hajnal, J., Jenkinson, M., Glocker, B., Rueckert, D., 2018. Multimodal surface matching with higher-order smoothness constraints. Neuroimage 167, 453-465.

Sadato, N., Morita, K., Kasai, K., Fukushi, T., Nakamura, K., Nakazawa, E., Okano, H., Okabe, S., 2019. Neuroethical Issues of the Brain/MINDS Project of Japan. Neuron 101, 385-389.

Salimi-Khorshidi, G., Douaud, G., Beckmann, C.F., Glasser, M.F., Griffanti, L., Smith, S.M., 2014. Automatic denoising of functional MRI data: combining independent component analysis and hierarchical fusion of classifiers. Neuroimage 90, 449-468.

Schmaal, L., Hibar, D.P., Samann, P.G., Hall, G.B., Baune, B.T., Jahanshad, N., Cheung, J.W., van Erp, T.G.M., Bos, D., Ikram, M.A., Vernooij, M.W., Niessen, W.J., Tiemeier, H., Hofman, A., Wittfeld, K., Grabe, H.J., Janowitz, D., Bulow, R., Selonke, M., Volzke, H., Grotegerd, D., Dannlowski, U., Arolt, V., Opel, N., Heindel, W., Kugel, H., Hoehn, D., Czisch, M., Couvy-Duchesne, B., Renteria, M.E., Strike, L.T., Wright, M.J., Mills, N.T., de Zubicaray, G.I., McMahon, K.L., Medland, S.E., Martin, N.G., Gillespie, N.A., Goya-Maldonado, R., Gruber, O., Kramer, B., Hatton, S.N., Lagopoulos, J., Hickie, I.B., Frodl, T., Carballedo, A., Frey, E.M., van Velzen, L.S., Penninx, B., van Tol, M.J., van der Wee, N.J., Davey, C.G., Harrison, B.J., Mwangi, B., Cao, B., Soares, J.C., Veer, I.M., Walter, H., Schoepf, D., Zurowski, B., Konrad, C., Schramm, E., Normann, C., Schnell, K., Sacchet, M.D., Gotlib, I.H., MacQueen, G.M., Godlewska, B.R., Nickson, T., McIntosh, A.M., Papmeyer, M., Whalley, H.C., Hall, J., Sussmann, J.E., Li, M., Walter, M., Aftanas, L., Brack, I., Bokhan, N.A., Thompson, P.M., Veltman, D.J., 2017. Cortical abnormalities in adults and adolescents with major depression based on brain scans from 20 cohorts worldwide in the ENIGMA Major Depressive Disorder Working Group. Mol Psychiatry 22, 900-909.

Schmaal, L., Veltman, D.J., van Erp, T.G., Samann, P.G., Frodl, T., Jahanshad, N., Loehrer, E., Tiemeier, H., Hofman, A., Niessen, W.J., Vernooij, M.W., Ikram, M.A., Wittfeld, K., Grabe, H.J., Block, A., Hegenscheid, K., Volzke, H., Hoehn, D., Czisch, M., Lagopoulos, J., Hatton, S.N., Hickie, I.B., Goya-Maldonado, R., Kramer, B., Gruber, O., Couvy-Duchesne, B., Renteria, M.E., Strike, L.T., Mills, N.T., de Zubicaray, G.I., McMahon, K.L., Medland, S.E., Martin, N.G., Gillespie, N.A., Wright, M.J., Hall, G.B., MacQueen, G.M., Frey, E.M., Carballedo, A., van Velzen, L.S., van Tol, M.J., van der Wee, N.J., Veer, I.M., Walter, H., Schnell, K., Schramm, E., Normann, C., Schoepf, D., Konrad, C., Zurowski, B., Nickson, T., McIntosh, A.M., Papmeyer, M., Whalley, H.C., Sussmann, J.E., Godlewska, B.R., Cowen, P.J., Fischer, F.H., Rose, M., Penninx, B.W., Thompson, P.M., Hibar, D.P., 2016. Subcortical brain alterations in major depressive disorder: findings from the ENIGMA Major Depressive Disorder working group. Mol Psychiatry 21, 806-812.

Setsompop, K., Gagoski, B.A., Polimeni, J.R., Witzel, T., Wedeen, V.J., Wald, L.L., 2012. Blipped-controlled aliasing in parallel imaging for simultaneous multislice echo planar imaging with reduced g-factor penalty. Magn Reson Med 67, 1210-1224.

Smith, S.M., Nichols, T.E., Vidaurre, D., Winkler, A.M., Behrens, T.E., Glasser, M.F., Ugurbil, K., Barch, D.M., Van Essen, D.C., Miller, K.L., 2015. A positive-negative mode of population covariation links brain connectivity, demographics and behavior. Nat Neurosci 18, 1565-1567.

Somerville, L.H., Bookheimer, S.Y., Buckner, R.L., Burgess, G.C., Curtiss, S.W., Dapretto, M., Elam, J.S., Gaffrey, M.S., Harms, M.P., Hodge, C., Kandala, S., Kastman, E.K., Nichols, T.E., Schlaggar, B.L., Smith, S.M., Thomas, K.M., Yacoub, E., Van Essen, D.C., Barch, D.M., 2018. The Lifespan Human Connectome Project in Development: A large-scale study of brain connectivity development in 5-21 year olds. Neuroimage 183, 456-468.

Sotiropoulos, S.N., Hernandez-Fernandez, M., Vu, A.T., Andersson, J.L., Moeller, S., Yacoub, E., Lenglet, C., Ugurbil, K., Behrens, T.E.J., Jbabdi, S., 2016. Fusion in diffusion MRI for improved fibre orientation estimation: An application to the 3T and 7T data of the Human Connectome Project. Neuroimage 134, 396-409.

Tong, Q., He, H., Gong, T., Li, C., Liang, P., Qian, T., Sun, Y., Ding, Q., Li, K., Zhong, J., 2020. Multicenter dataset of multi-shell diffusion MRI in healthy traveling adults with identical settings. Sci Data 7, 157.

van Erp, T.G., Hibar, D.P., Rasmussen, J.M., Glahn, D.C., Pearlson, G.D., Andreassen, O.A., Agartz, I., Westlye, L.T., Haukvik, U.K., Dale, A.M., Melle, I., Hartberg, C.B., Gruber, O., Kraemer, B., Zilles, D., Donohoe, G., Kelly, S., McDonald, C., Morris, D.W., Cannon, D.M., Corvin, A., Machielsen, M.W., Koenders, L., de Haan, L., Veltman, D.J., Satterthwaite, T.D., Wolf, D.H., Gur, R.C., Gur, R.E., Potkin, S.G., Mathalon, D.H., Mueller, B.A., Preda, A., Macciardi, F., Ehrlich, S., Walton, E., Hass, J., Calhoun, V.D., Bockholt, H.J., Sponheim, S.R., Shoemaker, J.M., van Haren, N.E., Hulshoff Pol, H.E., Ophoff, R.A., Kahn, R.S., Roiz-Santianez, R., Crespo-Facorro, B., Wang, L., Alpert, K.I., Jonsson, E.G., Dimitrova, R., Bois, C., Whalley, H.C., McIntosh, A.M., Lawrie, S.M., Hashimoto, R., Thompson, P.M., Turner, J.A., 2016. Subcortical brain volume abnormalities in 2028 individuals with schizophrenia and 2540 healthy controls via the ENIGMA consortium. Mol Psychiatry 21, 547-553.

Van Essen, D.C., Ugurbil, K., Auerbach, E., Barch, D., Behrens, T.E., Bucholz, R., Chang, A., Chen, L., Corbetta, M., Curtiss, S.W., Della Penna, S., Feinberg, D., Glasser, M.F., Harel, N., Heath, A.C., Larson-Prior, L., Marcus, D., Michalareas, G., Moeller, S., Oostenveld, R., Petersen, S.E., Prior, F., Schlaggar, B.L., Smith, S.M., Snyder, A.Z., Xu, J., Yacoub, E., Consortium, W.U.-M.H., 2012. The Human Connectome Project: a data acquisition perspective. Neuroimage 62, 2222-2231.

Wang, Y., Xu, Q., Luo, J., Hu, M., Zuo, C., 2019. Effects of Age and Sex on Subcortical Volumes. Front Aging Neurosci 11, 259.

Weiner, M.W., Veitch, D.P., Aisen, P.S., Beckett, L.A., Cairns, N.J., Cedarbaum, J., Green, R.C., Harvey, D., Jack, C.R., Jagust, W., Luthman, J., Morris, J.C., Petersen, R.C., Saykin, A.J., Shaw, L., Shen, L., Schwarz, A., Toga, A.W., Trojanowski, J.Q., Alzheimer's Disease Neuroimaging, I., 2015. 2014

Update of the Alzheimer's Disease Neuroimaging Initiative: A review of papers published since its inception. Alzheimers Dement 11, e1-120.

Winter, W., Sheridan, M., 2014. Previous reward decreases errors of commission on later 'No-Go' trials in children 4 to 12 years of age: evidence for a context monitoring account. Dev Sci 17, 797-807.

Xu, J., Moeller, S., Auerbach, E.J., Strupp, J., Smith, S.M., Feinberg, D.A., Yacoub, E., Ugurbil, K., 2013. Evaluation of slice accelerations using multiband echo planar imaging at 3 T. Neuroimage 83, 991-1001.

Yahata, N., Morimoto, J., Hashimoto, R., Lisi, G., Shibata, K., Kawakubo, Y., Kuwabara, H., Kuroda, M., Yamada, T., Megumi, F., Imamizu, H., Nanez, J.E., Sr., Takahashi, H., Okamoto, Y., Kasai, K., Kato, N., Sasaki, Y., Watanabe, T., Kawato, M., 2016. A small number of abnormal brain connections predicts adult autism spectrum disorder. Nat Commun 7, 11254.

Yamashita, A., Yahata, N., Itahashi, T., Lisi, G., Yamada, T., Ichikawa, N., Takamura, M., Yoshihara, Y., Kunimatsu, A., Okada, N., Yamagata, H., Matsuo, K., Hashimoto, R., Okada, G., Sakai, Y., Morimoto, J., Narumoto, J., Shimada, Y., Kasai, K., Kato, N., Takahashi, H., Okamoto, Y., Tanaka, S.C., Kawato, M., Yamashita, O., Imamizu, H., 2019. Harmonization of resting-state functional MRI data across multiple imaging sites via the separation of site differences into sampling bias and measurement bias. PLoS Biol 17, e3000042.

Zhang, H., Schneider, T., Wheeler-Kingshott, C.A., Alexander, D.C., 2012. NODDI: practical in vivo neurite orientation dispersion and density imaging of the human brain. Neuroimage 61, 1000-1016.